

Bayesian Controlled FDR Variable Selection via Knockoffs

Lorenzo Focardi-Olmi^{*†}, Anna Gottard[‡], Michele Guindani[‡] and Marina Vannucci^{*§}

November 6, 2024

Abstract

In many research fields, researchers aim to identify significant associations between a set of explanatory variables and a response while controlling the false discovery rate (FDR). To this aim, we develop a fully Bayesian generalization of the classical model-X knockoff filter. Knockoff filter introduces controlled noise in the model in the form of cleverly constructed copies of the predictors as auxiliary variables. In our approach we consider the joint model of the covariates and the response and incorporate the conditional independence structure of the covariates into the prior distribution of the auxiliary knockoff variables. We further incorporate the estimation of a graphical model among the covariates, which in turn aids knockoffs generation and improves the estimation of the covariate effects on the response. We use a modified spike-and-slab prior on the regression coefficients, which avoids the increase of the model dimension as typical in the classical knockoff filter. Our model performs variable selection using an upper bound on the posterior probability of non-inclusion. We show how our model construction leads to valid model-X knockoffs and demonstrate that the proposed characterization is sufficient for controlling the BFDR at an arbitrary level, in finite samples. We also show that the model selection is robust to the estimation of the

^{*}Department of Statistics, Rice University, USA

[†]Department of Statistics, Computer Science, Application "G.Parenti", University of Florence, Italy

[‡]Department of Biostatistics, University of California at Los Angeles, USA

[§]Corresponding author: marina@rice.edu

precision matrix. We use simulated data to demonstrate that our proposal increases the stability of the selection with respect to classical knockoff methods, as it relies on the entire posterior distribution of the knockoff variables instead of a single sample. With respect to Bayesian variable selection methods, we show that our selection procedure achieves comparable or better performances, while maintaining control over the FDR. Finally, we show the usefulness of the proposed model with an application to real data.

Keywords: False Discovery Rate; Graphical Models; MCMC; Regression; Spike-and-Slab Priors

1 Introduction

In recent years, variable selection has emerged as a crucial task at the forefront of statistics and machine learning. Variable selection is becoming increasingly essential in scientific research, as it enables to search for associations between an outcome variable and a large amount of possible explanatory variables, despite only a few of them being truly relevant. Thus, the need for methods that can accurately identify the subset of variables that affect the outcome is paramount. Consequently, variable selection is a well-studied topic in the statistical literature, particularly in the regression context, where it reduces to the selection of the non-zero model coefficients. Classical approaches for variable selection typically rely on constrained optimization of the likelihood function (see, among others, Tibshirani, 1996; Fan and Li, 2001; Zou and Hastie, 2005). In the Bayesian approach, variable selection can be performed by employing different classes of prior distributions (Tadesse and Vannucci, 2021). For regression models, spike-and-slab priors, proposed for the first time by Mitchell and Beauchamp (1988), impose mixture distributions on the regression coefficients, with latent binary indicators that identify the active predictors (George and McCulloch, 1997; Brown et al., 1998). Another approach involves the use of shrinkage priors to adaptively shrink coefficients towards zero (Park and Casella, 2008; Carvalho et al., 2010).

A fundamental challenge in variable selection is controlling the False Discovery Rate

(FDR), to ensure the reliability and replicability of research findings. False discoveries refer to situations where a statistical procedure incorrectly identifies a variable as active when, in reality, its effect is merely due to random chance or noise in the data. Multiple testing procedures have been proposed (see, for instance, Benjamini and Hochberg, 1995; Benjamini and Yekutieli, 2001, 2005) that aim at controlling the average proportion of false discoveries. These procedures typically rely on computing p -values, which is not always an easy task (Candès et al., 2018). Alternative methodologies have been developed by Xing et al. (2023), who propose a method that leverages a pair of mirror variables for each predictor to provide asymptotic control on the FDR, and by Dai et al. (2022), who employ a data-splitting procedure to accomplish the same goal with minimal computational effort.

Certain classical techniques for FDR control reach their goal by introducing controlled perturbation to the data. Barber and Candès (2015) propose the *knockoff filter*, a powerful tool that effectively achieves finite sample FDR control in fixed design low dimensional linear models. The key idea is to add controlled noise in the form of cleverly constructed copies of the predictors. Subsequently, a standard linear model is fitted on the augmented design matrix, and variable selection is performed using a function of the coefficients of both the original and the knockoff variables. Basically, knockoff variables are used as negative controls. This idea is extended to the case of fixed design high dimensional linear models in Barber and Candès (2019). Since this approach relies on a fixed design matrix, it is called *fixed-X knockoff*. An extension of this setting is the so-called *model-X knockoff filter* (Candès et al., 2018), which does not assume as true any model on the relation between the response and the covariates. Instead, it requires a complete knowledge of the joint distribution of the covariates. Alternative perspectives have been investigated by Sesia et al. (2018), who provide an efficient exact sampling of the knockoff variables when the covariates are distributed as a hidden Markov model, and by Bates et al. (2021), who apply a modified version of the algorithm proposed by Candès et al. (2018) to sample knockoffs exactly in the case of known independence structure of the covariates. Finally, Berti et al. (2023) provide a new characterization of the joint distribution of the observed covariates and the knockoffs, which they define in terms of copulas. When the covariates follow a joint Gaussian distribution their approach provides the same solution as in Candès et al. (2018).

In Bayesian settings, the usual definition of FDR cannot be used, since both the set of active and inactive variables are considered random variables. Instead, the Bayesian FDR (BFDR) is defined as an expected FDR conditionally upon the observed data, that is as the expected proportion of incorrect rejections among all possible rejections, computed with respect to the posterior distribution of active/inactive variables conditioned upon the observed data (Muller et al., 2006; Whittmore, 2007). An advantage of Bayesian methods is that they can facilitate multiplicity adjustments through the choice of the prior. For example, in the context of variable selection, Scott and Berger (2010) show that a spike-and-slab prior with a Beta-Bernoulli prior on the selection indicator achieves an asymptotic multiplicity control. Muller et al. (2006) and Guindani et al. (2009) prove control of the Bayesian FDR by characterizing the FDR problem as a decision problem where the optimal decision rule is based on thresholding the marginal posterior probabilities. More recently, Castillo and Roquain (2020) prove control of the Bayes FDR for general empirical Bayes multiple testing procedures. In practical settings, the optimal threshold for controlling the FDR corresponds to the minimum marginal probability of inclusion that ensures that the BFDR is less than the desired level (Newton et al., 2004). Therefore, this procedure relies on the estimates of these probabilities, as obtained from the MCMC output.

In this work, we develop a fully Bayesian generalization of the model-X knockoff filter. One of the main issues of the classical model-X knockoff filter is that the inference process concerning the set of active variables heavily relies on the quality of the randomly generated sample of knockoff variables. As a result, the procedure may exhibit instability and produce different sets of active variables for the same set of predictors. To mitigate this issue, Ren et al. (2023) combine the knockoff filter with the stability selection procedure of Meinshausen and Bühlmann (2010), obtaining improved inference and a more stable selection of active variables. This issue of stability is naturally addressed within the Bayesian framework, where the knockoffs variables are treated as latent and updated as part of the posterior inference. In particular, in our proposed approach, we consider the joint model of the covariates and the response and incorporate the conditional independence structure of the covariates into the prior distribution of the knockoff variables. Our joint modeling construction employs a likelihood decomposition via auxiliary variables that allows us to obtain valid model-X

knockoffs. We further assume a Gaussian graphical model on the covariates and impose the continuous spike-and-slab prior of Wang (2015) on the precision matrix. Estimating a graphical model on the covariates allows us to obtain a coherent model which does not require perfect knowledge of the precision matrix. Moreover, differently from any plug-in estimator, we can incorporate prior information about the conditional dependence structure of the covariates into the model, assuring a better knockoff quality, as argued by Barber et al. (2020). For the regression coefficients, we follow a suggestion from Candès et al. (2018) and assume a mixture of spike-and-slab prior, which avoids the increase of the model dimension typical with the classical knockoff filter, and which we further modify by letting the probability of inclusion of a variable depend on the number of its neighbors in the graph. We ensure that the knockoff variables possess *a priori* the required properties outlined in Candès et al. (2018) and demonstrate that this characterization is sufficient for controlling the BFDR at an arbitrary level, in finite samples. Moreover, for a sufficiently large sample size, we prove that FDR control is achieved even without the knowledge of the true covariates' graph. In applications, to maintain control over the BFDR, we employ a greedy algorithm, similar to the one presented in Newton et al. (2004), but relying on an estimate of the upper bound for the probability of non-inclusion. We use simulated data to demonstrate that our proposal increases the stability of the selection with respect to classical knockoff methods, as it relies on the entire posterior distribution of the knockoff variables instead of a single sample. With respect to Bayesian variable selection methods, we show that our selection procedure achieves comparable or better performances, while maintaining control over the FDR.

Very few attempts have been made at constructing Bayesian knockoffs filters. Gu and Yin (2021) first considered a generalized linear model framework and assumed the distribution of the covariates to be completely known. With respect to their model formulation, in our approach the incorporation of the estimation of a graphical model on the covariates aids knockoffs generation and improves the estimation of the covariate effects on the response. Furthermore, unlike the model formulation of Gu and Yin (2021), our joint model ensures valid model-X knockoffs. Yap and Gauran (2023) employ the Bayesian lasso of Park and Casella (2008) for the estimation of the regression coefficients. However, they treat the

covariates as fixed and assume that the augmented knockoff matrix is generated before the application of the Bayesian method.

The paper is organized as follows. Section 2 provides an overview of the fundamental concepts related to knockoff filters and introduces the proposed Bayesian generalization. Section 3 presents a comprehensive simulation study to evaluate the performances of the proposed method against alternative approaches. Section 4 uses an application to real data to demonstrate the practical utility of our approach. Some concluding remarks are presented in Section 5.

2 Methods

Let $X = (X_1, \dots, X_p)$ be a set of covariates and Y a response variable. We observe i.i.d. data assembled in an $(n \times p)$ data matrix $\mathbf{X} = (x_1, \dots, x_n)$ and an n -dimensional vector $y = (y_1, \dots, y_n)$. In this section, we first introduce the classical notion of knockoff filters for the linear regression framework and then describe our proposed Bayesian generalization.

2.1 Knockoff filter

Knockoff filter is a framework that enables variable selection in an FDR-controlled environment. The main idea, originally proposed by Barber and Candès (2015), is to perturb the model by adding a set of inactive predictors built in such a way that they resemble the dependence structure of the original covariates. In Barber and Candès (2015) the knockoff predictors were built deterministically, while Candès et al. (2018) extended the framework to the model- X knockoff filter, with random covariates. The model- X knockoff assumes a joint distribution $p(X)$ for the predictors and random knockoff variables, $\tilde{X} = (\tilde{X}_1, \dots, \tilde{X}_p)^T$, which are defined in a way to make it hard for the model to distinguish them from X . Formally, the knockoffs are sampled from a distribution $p(\tilde{X} | X)$ such that these two properties hold:

1. Conditional Independence:

$$\tilde{X} \perp\!\!\!\perp Y | X$$

2. Pairwise Exchangeability:

$$(X, \tilde{X})_{\text{Swap}(j)} \stackrel{d}{=} (X, \tilde{X}) \quad j = 1, \dots, p,$$

where $(X, \tilde{X})_{\text{Swap}(j)}$ results from swapping the j -th variable with the j -th knockoff. Note that while the first property is easily obtained, the second presents some difficulties (Sesia et al., 2018; Bates et al., 2021; Berti et al., 2023). A general algorithm to sample knockoffs is given in Candès et al. (2018), but it requires the computation of the conditional probability distribution of each covariate given all the others and the previously sampled knockoffs, $p(X_j | X_{\setminus j}, \tilde{X}_{1:j-1})$, which can be difficult to obtain for general distributions. On the other hand, when all covariates are pairwise independent, each knockoff can be sampled from the marginal distribution of X_j .

In the classical knockoff framework as proposed by Barber and Candès (2015), given the sampled knockoff variables $\tilde{\mathbf{X}} = (\tilde{x}_1, \dots, \tilde{x}_n)$, any model which returns a variable importance metric is fit using the augmented set of predictors $[\mathbf{X}, \tilde{\mathbf{X}}]$. Variable selection is performed by defining a feature statistic W_j , $j = 1, \dots, p$, which combines the variable importance metric of each original predictor with the one of its own knockoff, using any antisymmetric function such that it has a symmetric distribution around zero for inactive variables. The final set of selected variables consists of those exceeding a pre-defined threshold, chosen according to a desired FDR level.

The procedure of model-X knockoffs (Candès et al., 2018) described above can be simplified if the distribution of the covariates is Gaussian. Let $X \sim N(0, \Sigma)$, with Σ the covariance matrix, then a joint distribution for which pairwise exchangeability holds is

$$(X, \tilde{X}) \sim N \left(0, \begin{pmatrix} \Sigma & \Sigma - \text{diag}(s) \\ \Sigma - \text{diag}(s) & \Sigma \end{pmatrix} \right), \quad (1)$$

where $s = (s_1, \dots, s_p)^T$ is a vector of values computed by minimizing the average correlation between each variable and its knockoff while ensuring that

$$A = 2\text{diag}(s) - \text{diag}(s)\Sigma^{-1}\text{diag}(s) \quad (2)$$

is positive definite. Thus, by the property of the multivariate distribution, the conditional distribution of the knockoffs \tilde{X} given the covariates X is obtained as follows

$$\tilde{X} | X \sim N(X - X\Sigma^{-1}\text{diag}(s), \mathbf{A}). \quad (3)$$

Note that Equation (3) implies

$$\tilde{X} = X(I - \Sigma^{-1}\text{diag}(s)) + U. \quad (4)$$

with $U \sim N(0, A)$.

2.2 Bayesian knockoffs

We now introduce our Bayesian generalization of the model-X knockoff filter. We are interested in the joint model for Y, X , e.g. $p(Y, X)$. In particular, our interest focuses on the elements of the factorization of $p(Y, X)$ into the conditional distribution $p(Y|X)$ and the marginal distribution $p(X)$. For the latter we assume a multivariate Gaussian model as

$$X \sim N(0, \Sigma), \quad (5)$$

which implies that the joint distribution of (X, \tilde{X}) is as reported in Equation (1). We then derive the conditional distribution $p(Y | X)$ as the marginal distribution over the knockoff variables \tilde{X} of the distribution $p(Y | X, \tilde{X})$ as

$$p(Y | X) = \int p(Y | X, \tilde{X})p(\tilde{X} | X)d\tilde{X}. \quad (6)$$

We consider a linear regression setting, where we aim at simultaneously inferring the subset of active predictors while also learning the conditional independence structure of the covariates. Thus, we specify the distribution $p(Y | X, \tilde{X})$ as a linear regression model of the type

$$Y = X\beta + \tilde{X}\tilde{\beta} + \epsilon, \quad \epsilon \sim N(0, \sigma^2), \quad (7)$$

where β and $\tilde{\beta}$ are p -dimensional vectors of the covariates' effects and the knockoffs' effects on Y , respectively. Following the decomposition introduced in Equation (4), we can rewrite the model in Equation (7) as

$$Y = X[\beta + (I_p - \mathbf{\Omega}\text{diag}(s))\tilde{\beta}] + U\tilde{\beta} + \epsilon, \quad \epsilon \sim N(0, \sigma^2), \quad (8)$$

where $\mathbf{\Omega} = \mathbf{\Sigma}^{-1}$ is the precision matrix. Under this specification, it is possible to obtain the target distribution $p(Y | X)$ in closed form as

$$p(Y | X) = \int p(Y | X, U)p(U)dU = N(X(\beta + (I_p - \mathbf{\Omega}\text{diag}(s))\tilde{\beta}), I_n(\tilde{\beta}^T A \tilde{\beta} + \sigma^2)), \quad (9)$$

with the matrix A as defined in Equation (2). This construction respects the conditional independence property of the knockoff variables, as now $Y \perp\!\!\!\perp \tilde{X} | X$. Moreover, since the decomposition of the knockoff variables in Equation (4) is obtained from the joint distribution in Equation (1), our formulation respects the pairwise exchangeability too. Therefore, this setting uses valid model- X knockoffs.

2.2.1 Sparsity inducing prior for covariates' graphical model

We regard the Gaussian distribution (5) on the covariates as a graphical model and impose sparsity in the associated graph structure. Under the assumption of joint Gaussian distribution, conditional independence implies zero values in the off-diagonal elements of the precision matrix $\mathbf{\Omega} = \mathbf{\Sigma}^{-1}$. When $\mathbf{\Omega}$ is sparse, also the matrix \mathbf{A} in Equation (2) is sparse, facilitating the sampling of the knockoff variables under the pairwise exchangeability property. In addition, promoting sparsity in the precision matrix $\mathbf{\Omega}$ greatly improves computational efficiency and improves practical interpretability across various application domains. Here, we achieve this by imposing a continuous spike-and-slab prior (Wang, 2015) that combines a mixture prior distribution on the off-diagonal elements $\omega_{jj'}$ with an exponential distribution on the diagonal ones ω_{jj} ($j = 1, \dots, p$). Let \mathcal{G} be the undirected graph representing the conditional independences among the covariates, and let \mathbf{G} be the adjacency matrix with elements $g_{jj'} \in \{0, 1\}$, for $j, j' = 1, \dots, p$ and $j \neq j'$, with 1 representing the presence of an

edge between nodes (j, j') . Assuming the parameters in $\boldsymbol{\Omega}$ independent a priori, the prior distribution can be written as

$$p(\boldsymbol{\Omega} \mid \mathbf{G}, v_0, v_1, \theta) = \frac{1}{K(\mathbf{G}, v_0, v_1, \theta)} \prod_{j < j'} N(\omega_{jj'} \mid 0, v_{g_{jj'}}) \prod_j \text{Exp}(\omega_{jj} \mid \theta/2), \quad (10)$$

where $K(\mathbf{G}, v_0, v_1, \theta)$ is the normalizing constant, and where $v_{g_{jj'}} \in \{v_0, v_1\}$, with v_0 the variance of the Gaussian distribution for the absence of an edge and v_1 the variance of the edge presence. By setting a small value for v_0 in the continuous spike-and-slab prior, we ensure that the entries of the precision matrix $\boldsymbol{\Omega}$ corresponding to non-selected edges are close to zero. As we will see in the next section, the graphical structure is used to inform variable selection in a way that improves performances. We complete the prior by assuming independent probabilities of selecting edges as

$$p(\mathbf{G} \mid v_0, v_1, \theta, \xi) = \frac{K(\mathbf{G}, v_0, v_1, \theta)}{K(v_0, v_1, \xi)} \prod_{j < j'} \xi^{g_{jj'}} (1 - \xi)^{1 - g_{jj'}}, \quad (11)$$

where $K(v_0, v_1, \xi)$ is the normalizing constant of the distribution and ξ is the prior probability of edge inclusion.

2.2.2 Priors for variable selection

For the regression coefficients, we consider a modified spike-and-slab prior distribution similar to the one introduced in the supplementary material of Candès et al. (2018). This prior is specified as the joint distribution

$$p(\beta_j, \tilde{\beta}_j \mid h_\beta, \boldsymbol{\gamma}, \sigma^2) = \begin{cases} \delta_0(\beta_j, \tilde{\beta}_j) & \text{w.p. } \mathbb{P}[\gamma_j = 0] \\ N(\beta_j \mid 0, h_\beta \sigma^2) \delta_0(\tilde{\beta}_j) & \text{w.p. } \mathbb{P}[\gamma_j = 1]/2 \\ \delta_0(\beta_j) N(\tilde{\beta}_j \mid 0, h_\beta \sigma^2) & \text{w.p. } \mathbb{P}[\gamma_j = 1]/2, \end{cases} \quad (12)$$

with $j = 1, \dots, p$. Here, h_β is a fixed positive scaling hyperparameter and $\boldsymbol{\gamma} = (\gamma_1, \dots, \gamma_p)^T \in \{0, 1\}^p$ is a p -dimensional vector of binary indicators such that $\gamma_j = 1$ if X_j or its knockoff \tilde{X}_j are included in the model and, alternatively, $\gamma_j = 0$ if neither the original feature nor the

knockoff is included. By introducing two additional latent indicator vectors, $\delta = (\delta_1, \dots, \delta_p)$ and $\tilde{\delta} = (\tilde{\delta}_1, \dots, \tilde{\delta}_p)$, such that $\gamma = \delta + \tilde{\delta}$, the joint prior in Equation (12) can be reformulated as a mixture of independent spike-and-slab priors on β_j and $\tilde{\beta}_j$ as

$$p\left(\beta_j, \tilde{\beta}_j \mid h_\beta, \delta_j, \tilde{\delta}_j, \sigma^2\right) = \delta_j N\left(\beta_j \mid 0, h_\beta \sigma^2\right) \delta_0(\tilde{\beta}_j) + \tilde{\delta}_j N\left(\tilde{\beta}_j \mid 0, h_\beta \sigma^2\right) \delta_0(\beta_j) + (1 - \delta_j - \tilde{\delta}_j) \delta_0(\beta_j, \tilde{\beta}_j).$$

Including both a covariate and its knockoff simultaneously in the model would introduce bias in the regression coefficient estimates. Therefore, we do not allow both indicators to assume value 1 and choose a multinomial distribution of the type

$$\left(\delta_j, \tilde{\delta}_j\right) \mid \gamma \sim \begin{cases} (0, 0) & \text{w.p. } \mathbb{P}[\gamma_j = 0] \\ (0, 1) & \text{w.p. } \mathbb{P}[\gamma_j = 1]/2 \\ (1, 0) & \text{w.p. } \mathbb{P}[\gamma_j = 1]/2. \end{cases}$$

Furthermore, we let the probability of success depend on the graphical model on the covariates, similar to Peterson et al. (2016), via an Ising prior of the type

$$p(\gamma \mid \mathbf{G}, a, b) \propto \exp\left(a \mathbf{1}^T \gamma + b \gamma^T \mathbf{G} \gamma\right), \quad (13)$$

where \mathbf{G} is the adjacency matrix of the undirected graph on the covariates. The hyperparameter a controls the overall sparsity of the vector γ , while b is linked to the graph influence on the selection. Specifically, increasing the value of b increases the probability to have $\gamma_j = 1$ for the variables with many edges in the graph. Lastly, we complete our prior model with a conjugate prior on the variance σ^2 ,

$$\sigma^2 \sim \text{IG}(a_\sigma, b_\sigma). \quad (14)$$

We note that Candès et al. (2018) adopt prior in Equation (12) in a fixed design Bayesian regression with augmented covariates matrix $[\mathbf{X}, \tilde{\mathbf{X}}]$ where $\tilde{\mathbf{X}}$ is sampled once from Equation (3). On the contrary, we consider the knockoffs as latent variables and update them in

the posterior sampling along with the other parameters.

2.2.3 Markov Chain Monte Carlo for posterior sampling

Let $\mathbf{D} = \{x_i, y_i\}_{i=1}^n$ represent the sample data and let Θ indicate the set of unknown model parameters and latent variables, $\Theta = \{\beta, \tilde{\beta}, \sigma^2, \delta, \tilde{\delta}, \gamma, \mathbf{\Omega}, \mathbf{G}\}$. The joint posterior distribution is proportional to the product between the likelihood and the prior distributions

$$p(\Theta | \mathbf{D}) \propto p(Y | X, \Theta) p(X | \Theta) p(\Theta) \propto p(Y | X, \beta, \tilde{\beta}, \mathbf{\Omega}, \sigma^2) p(X | \mathbf{\Omega}) p(\beta, \tilde{\beta} | \delta, \tilde{\delta}) p(\delta, \tilde{\delta} | \gamma) p(\mathbf{\Omega} | \mathbf{G}) p(\gamma | \mathbf{G}) p(\mathbf{G}) p(\sigma^2).$$

This distribution is not analytically tractable, and we therefore resort to a Markov Chain Monte Carlo (MCMC) algorithm (Brooks et al., 2011). In particular, we implement an efficient Metropolis within Gibbs scheme that employs a data augmentation (DA) scheme based on the latent variable U introduced in (4) and the formulation of the joint model detailed in Section 2.2. Specifically, as it is not possible to obtain tractable full conditional distributions using the marginal model $p(Y | X, \beta, \tilde{\beta}, \mathbf{\Omega}, \sigma^2)$, we employ a DA step by sampling from the distribution $p(Y | X, U, \beta, \tilde{\beta}, \mathbf{\Omega}, \sigma^2)$ defined in Equation (8) and then updating U from the full conditional. We also incorporate the Add-Delete Metropolis-Hastings algorithm of Savitsky et al. (2011), that cleverly avoids having to deal with the changing dimensions of the parameter space via a joint update of the inclusion indicators of the spike-and-slab priors and the corresponding regression coefficients. In practice, our algorithm is composed by the following steps:

1. We jointly update $(\delta, \tilde{\delta}, \gamma, \beta, \tilde{\beta})$ with a stochastic search approach. At each iteration $t = 1, \dots, T$, we randomly select one $j \in \{1, \dots, p\}$ and propose to change the value of γ_j . If the proposed $\gamma_j^* = 0$ then the only possible choice for the proposed $\beta_j^*, \tilde{\beta}_j^*, \delta_j^*, \tilde{\delta}_j^*$ is to set them all to 0. However, if we select a non-included variable, $\gamma_j = 0$, we randomly propose to include the original variable or its knockoff. More specifically, we propose the selected coefficient using a Gaussian distribution $N(0, 0.5)$ as the proposal

distribution. We then accept the proposed parameters with probability

$$r = \min \left\{ 1, \frac{p(Y | X, U, \beta^*, \tilde{\beta}^*, \mathbf{\Omega}, \sigma^2)p(\beta^*, \tilde{\beta}^* | \gamma^*, \sigma^2, h_\beta)p(\delta^*, \tilde{\delta}^* | \gamma^*)p(\gamma^* | \mathbf{G}, a, b)}{p(Y | X, U, \beta, \tilde{\beta}, \mathbf{\Omega}, \sigma^2)p(\beta, \tilde{\beta} | \gamma, \sigma^2, h_\beta)p(\delta, \tilde{\delta} | \gamma)p(\gamma | \mathbf{G}, a, b)} \right\}$$

To improve the mixing of the algorithm, we perform a within-model update step, proposing a new value for each selected coefficient using as proposal a distribution centered on the current value of $(\beta, \tilde{\beta})$.

2. We sample σ^2 from its full conditional distribution

$$\sigma^2 | y, \mathbf{X}, U, \beta, \tilde{\beta}, \mathbf{\Omega} \sim IG \left(a_\sigma + \frac{n}{2}, b_\sigma + \frac{\sum_i (y_i - x_i[\beta + (I - \mathbf{\Omega}\text{diag}(s))\tilde{\beta}] - U_i\tilde{\beta})^2}{2} \right).$$

3. The update of \mathbf{G} and $\mathbf{\Omega}$ is done via a block Gibbs sampler similar to the one used by Wang (2015).
4. Lastly, we update the elements of the latent auxiliary variable U from their full conditional distributions

$$\begin{aligned} u_i | y, \mathbf{X}, U, \beta, \tilde{\beta}, \mathbf{\Omega}, \sigma^2 &\sim N(\mu_i, \Sigma_U) \\ \Sigma_U &= \left(A + \frac{1}{\sigma^2} \tilde{\beta} \tilde{\beta}^T \right)^{-1} \\ \mu_i &= \Sigma_U \left(\frac{1}{\sigma^2} \left(y_i \tilde{\beta} - \tilde{\beta} \beta^T x_i - \tilde{\beta} \tilde{\beta}^T \Gamma_i \right) \right) \\ \Gamma &= X(I - \mathbf{\Omega}\text{diag}(s)), \end{aligned}$$

for $i = 1, \dots, n$.

2.3 Controlling the false discovery rate

In this section, we demonstrate that our model effectively performs variable selection while controlling the Bayesian FDR. In Bayesian frameworks, the conventional definition of the false discovery rate is not directly applicable, as both the set of active and inactive variables are treated as random variables. To address this, it is customary to rely on a notion of

Bayesian FDR, as discussed for example by Whittemore (2007), where it is defined as the expected value of the false discovery proportion conditioned on the observed data, \mathbf{D} , as

$$BFDR(\mathcal{S}) = \mathbb{E} \left[\frac{|\{j \in \mathcal{S} : X_j \perp\!\!\!\perp Y\}|}{|\mathcal{S}| \vee 1} \mid \mathbf{D} \right], \quad (15)$$

where $\mathcal{S} \subseteq \{1, \dots, p\}$ is the subset of selected indexes. Thus, the BFDR represents the expected proportion of incorrect rejections among all possible rejections, where the expectation is conditioned on the posterior distribution of active and inactive variables given the observed data. Proposition 1 states that, given an antisymmetric function W_j , our proposed method controls the BFDR at level q .

Proposition 1. *Let the prior distribution for the knockoff latent variable U be such that pairwise exchangeability holds, i.e.*

$$p(X, \tilde{X})_{\text{Swap}(j)} = p(X, \tilde{X}) \quad \forall j \in \{1, \dots, p\}.$$

Let the distribution of the response variable Y follow the model in Equation (9) with prior distribution on the regression coefficient invariant to swaps, i.e.

$$p(\beta, \tilde{\beta})_{\text{Swap}(j)} = p(\beta, \tilde{\beta}) \quad j \in \{1, \dots, p\}.$$

Then, the set $\hat{\mathcal{S}} = \arg \max_{\mathcal{S} \subseteq \{1, \dots, p\}} |\mathcal{S}|$ subject to

$$\frac{1}{|\mathcal{S}| \vee 1} \sum_{j \in \mathcal{S}} \{1 - \mathbb{P}[W_j > 0 \mid \mathbf{D}] + \mathbb{P}[W_j < 0 \mid \mathbf{D}]\} \leq q,$$

where $W(\beta, \tilde{\beta})$ is an antisymmetric function, controls the BFDR at level q .

Proof. Let $r = (r_1, \dots, r_p) \in \{0, 1\}^p$ be a random vector such that $r_j = 1 \iff X_j \perp\!\!\!\perp Y \mid X_{-j}$ with $X_{-j} = (X_1, \dots, X_{j-1}, X_{j+1}, \dots, X_p)$. Under a compound loss function (Muller et al., 2006), the Bayesian FDR can be written as

$$BFDR(\mathcal{S}) = \frac{\sum_{j \in \mathcal{S}} \mathbb{P}[r_j = 0 \mid \mathbf{D}]}{|\mathcal{S}| \vee 1},$$

where $\mathbb{P}[r_j = 0 \mid \mathbf{D}]$ represents the marginal posterior probability of a covariate to be inactive. Assume for now that the random vector W satisfies the sign-flip property, i.e.

$$\mathbb{P}[W_j > 0 \mid \mathbf{D}, r_j = 0] = \mathbb{P}[W_j < 0 \mid \mathbf{D}, r_j = 0].$$

Moreover, by construction, we have that $\mathbb{P}[W_j > 0 \mid \mathbf{D}, r_j = 1] > \mathbb{P}[W_j < 0 \mid \mathbf{D}, r_j = 1]$. Therefore, marginally with respect to r_j , we obtain

$$\mathbb{P}[W_j > 0 \mid \mathbf{D}] > \mathbb{P}[W_j < 0 \mid \mathbf{D}].$$

By law of total probability, we can write

$$\begin{aligned} \mathbb{P}[W_j > 0 \mid \mathbf{D}] &= \mathbb{P}[W_j > 0 \mid \mathbf{D}, r_j = 0] \mathbb{P}[r_j = 0 \mid \mathbf{D}] \\ &\quad + \mathbb{P}[W_j > 0 \mid \mathbf{D}, r_j = 1] \mathbb{P}[r_j = 1 \mid \mathbf{D}]. \end{aligned}$$

Applying the same argument to $\mathbb{P}[W_j < 0 \mid \mathbf{D}]$ and using the sign-flip property of W , we obtain

$$\begin{aligned} \mathbb{P}[W_j > 0 \mid \mathbf{D}] - \mathbb{P}[W_j < 0 \mid \mathbf{D}] &= \mathbb{P}[r_j = 1 \mid \mathbf{D}] \times (\mathbb{P}[W_j > 0 \mid \mathbf{D}, r_j = 1] \\ &\quad - \mathbb{P}[W_j < 0 \mid \mathbf{D}, r_j = 1]). \end{aligned}$$

Then, we can conclude,

$$\mathbb{P}[W_j > 0 \mid \mathbf{D}] - \mathbb{P}[W_j < 0 \mid \mathbf{D}] \leq \mathbb{P}[r_j = 1 \mid \mathbf{D}]. \quad (16)$$

Since $\mathbb{P}[r_j = 0 \mid \mathbf{D}] = 1 - \mathbb{P}[r_j = 1 \mid \mathbf{D}]$, the inequality in Equation (16) provides an upper bound for $\mathbb{P}[r_j = 0 \mid \mathbf{D}]$, i.e.,

$$\mathbb{P}[r_j = 0 \mid \mathbf{D}] \leq 1 - \mathbb{P}[W_j > 0 \mid \mathbf{D}] + \mathbb{P}[W_j < 0 \mid \mathbf{D}]. \quad (17)$$

To complete the proof, we need to show that an invariant prior on $(\beta, \tilde{\beta})$ leads to a W that

satisfies the sign-flip property. This result can be obtained using a similar argument as in Theorem 1 of Gu and Yin (2021). We report the proof in Appendix A for completeness. \square

In practice, we can compute the upper bound for $\mathbb{P}[r_j = 0 \mid \mathbf{D}]$ in Equation (17) via Monte Carlo sampling given the MCMC output, as

$$\widehat{\mathbb{P}}[r_j = 0 \mid \mathbf{D}] \leq 1 - \frac{1}{T} \left(\sum_{t=1}^T \mathbb{1}_{\{W_j^{(t)} > 0\}} - \mathbb{1}_{\{W_j^{(t)} < 0\}} \right), \quad (18)$$

where T is the number of posterior samples. A simple algorithm to construct the set $\widehat{\mathcal{S}}$ required by Proposition 1 is to compute the upper bound in Equation (18) for each covariate and sort them such that the bounds are in ascending order. Then, add variables to the set until the average of the upper bounds is below q . The final selection is not sensitive to the choice of W_j . We adopt the typical function

$$W_j = \left| \beta_j \right| - \left| \widetilde{\beta}_j \right|$$

in all applications of this paper. We remark that our model performs variable selection using an upper bound on the posterior probability of non-inclusion. This strategy allows us to overcome issues with strong correlation structure among the covariates, which typically affect the state-of-art variable selection methods that rely on the estimated marginal posterior probabilities of inclusion (see Scenario 3 of our simulation study below). Our theoretical results, indeed, show that the bound used for our variable selection procedure is not affected by the dependency structure of the covariates.

Although the result in Proposition 1 proves how the method controls the BFDR below a threshold q , it assumes that the latent variables \widetilde{X} can be considered as valid knockoffs a priori. As stated by Candès et al. (2018), the construction of valid model-X knockoffs requires perfect knowledge of the covariates' distribution. However, our proposed model assumes that the covariates X follow a Gaussian distribution where the precision matrix is not known and it has to be estimated. Barber et al. (2020) prove how the knockoff procedure still controls the FDR under a threshold q if the precision matrix of the Gaussian model is correctly estimated. Similarly, we are able to prove that, under mild regularity conditions,

the priors chosen to estimate the Gaussian graphical model for the covariates produce a good estimate of the precision matrix. Thus, employing similar arguments as in Barber et al. (2020), we can conclude that, for large sample sizes, our procedure effectively controls the frequentist FDR and, consequently, the expected BFDR over replicated experiments (Guindani et al., 2009), even if the precision matrix is unknown. More precisely, we are able to prove that the posterior convergence rate of our estimator is the same as the one of the Bayesian graphical lasso. To show that, we first need to prove that our prior distribution assigns enough probability to values “close” to the true one.

Proposition 2. *Let the true precision matrix $\Omega_0 \in \mathcal{U}(\epsilon_0, l) = \{\Omega : |\{(i, j) : 1 \leq i < j \leq p, \omega_{ij} \neq 0\}| \leq l, 0 < \epsilon_0 \leq \text{eig}(\Omega)_1 < \text{eig}(\Omega)_p \leq \epsilon_0^{-1} < \infty\}$ for some $0 < \epsilon_0 < \infty$ and $0 \leq l \leq p(1 - p)/2$. Also assume that the prior distributions for the precision matrix Ω and the adjacency matrix \mathbf{G} are:*

$$p(\Omega | \mathbf{G}, v_0, v_1, \theta) = \frac{1}{K(\mathbf{G}, v_0, v_1, \theta)} \prod_{j < j'} N(\omega_{jj'} | 0, v_{g_{jj'}}) \prod_j \text{Exp}(\omega_{jj} | \theta/2)$$

with $v_{g_{ij}} \leq \frac{\|\Omega_0\|_\infty}{2 \log 2}$ and

$$p(\mathbf{G} | v_0, v_1, \theta, \xi) = \frac{K(\mathbf{G}, v_0, v_1, \theta)}{K(v_0, v_1, \xi)} \prod_{j < j'} \xi^{g_{jj'}} (1 - \xi)^{1 - g_{jj'}},$$

with $\xi < 0.5$. Then,

$$\Pi(B(p_{\Omega_0}, \epsilon_n)) \gtrsim (c\epsilon_n/p)^{p+l},$$

where $\Pi(\cdot)$ denotes the probability under the prior distribution, $B(p_{\Omega_0}, \epsilon_n) = \{p : K(p_{\Omega_0}, p_\Omega) \leq \epsilon_n^2, V(p_{\Omega_0}, p_\Omega) \leq \epsilon_n^2\}$ with $K(f, g) = \int f \log(f/g)$ and $V(f, g) = \int f \log^2(f/g)$ and p_{Ω_0} and p_Ω are the density function of $N(0, \Omega_0)$ and $N(0, \Omega)$ respectively.

Proof. Following the same argument of Theorem 3.1 in Banerjee and Ghosal (2015), we can show that

$$B(p_{\Omega_0}, \epsilon_n) \supset \{p_\Omega : \|\Omega - \Omega_0\|_\infty \leq c\epsilon_n/p\}.$$

Therefore, it is sufficient to obtain a lower bound for the subset. Moreover, the components of Ω are not independently distributed, since the prior of Ω is truncated to the set of positive

definite matrices. However, as a small neighborhood of $\Omega_0 \in \mathcal{U}(\epsilon_0, l)$ lies within the set of positive definite matrices, the truncation can only increase prior concentration of $B(p_{\Omega_0}, \epsilon_n)$. Therefore, we can pretend componentwise independence for the purpose of lower bounding the above prior probability. Then, the probability of interest is

$$\begin{aligned}
\Pi(\|\Omega_0 - \Omega\|_\infty \leq c\epsilon_n/p) &= \Pi(\max_{ij} |\omega_{ij} - \omega_{0,ij}| \leq c\epsilon_n/p) \\
&= \prod_{ij} \Pi(|\omega_{ij} - \omega_{0,ij}| \leq c\epsilon_n/p) \\
&= \prod_{i < j} \int_{c\epsilon_n/p - \omega_{0,ij}}^{c\epsilon_n/p + \omega_{0,ij}} \frac{1}{\sqrt{2\pi v_{g_{ij}}}} e^{-\frac{\omega_{ij}^2}{2v_{g_{ij}}}} d\omega_{ij} \\
&\quad \times \prod_{i=1}^p \int_{c\epsilon_n/p - \omega_{0,ii}}^{c\epsilon_n/p + \omega_{0,ii}} \frac{\theta}{2} e^{-\frac{\theta}{2}\omega_{ii}} d\omega_{ii}.
\end{aligned}$$

We now focus on the first integral. We obtain

$$\begin{aligned}
\int_{c\epsilon_n/p - \omega_{0,ij}}^{c\epsilon_n/p + \omega_{0,ij}} \frac{1}{\sqrt{2\pi v_{g_{ij}}}} e^{-\frac{\omega_{ij}^2}{2v_{g_{ij}}}} d\omega_{ij} &= 1 - \left[\int_{c\epsilon_n/p + \omega_{0,ij}}^{\infty} \frac{1}{\sqrt{2\pi v_{g_{ij}}}} e^{-\frac{\omega_{ij}^2}{2v_{g_{ij}}}} d\omega_{ij} \right. \\
&\quad \left. + \int_{\omega_{0,ij} - c\epsilon_n/p}^{\infty} \frac{1}{\sqrt{2\pi v_{g_{ij}}}} e^{-\frac{\omega_{ij}^2}{2v_{g_{ij}}}} d\omega_{ij} \right] \\
&\geq 1 - \exp\left\{ \frac{c\epsilon_n/p - \omega_{0,ij}}{2v_{g_{ij}}} \right\} \\
&\quad - \exp\left\{ \frac{-c\epsilon_n/p - \omega_{0,ij}}{2v_{g_{ij}}} \right\},
\end{aligned}$$

where the bound is obtained by Chernoff inequality. We need to show that

$$\lim_{\epsilon_n \rightarrow 0} \frac{c\epsilon_n/p}{1 - \exp\left\{ \frac{c\epsilon_n/p - \omega_{0,ij}}{2v_{g_{ij}}} \right\} - \exp\left\{ \frac{-c\epsilon_n/p - \omega_{0,ij}}{2v_{g_{ij}}} \right\}} = 0^+,$$

since this would imply

$$\begin{aligned} & \int_{c\epsilon_n/p-\omega_{0,ij}}^{c\epsilon_n/p+\omega_{0,ij}} \frac{1}{\sqrt{2\pi v_{g_{ij}}}} e^{-\frac{\omega_{ij}^2}{2v_{g_{ij}}}} d\omega_{ij} \\ & \geq 1 - \exp\left\{\frac{c\epsilon_n/p - \omega_{0,ij}}{2v_{g_{ij}}}\right\} - \exp\left\{\frac{-c\epsilon_n/p - \omega_{0,ij}}{2v_{g_{ij}}}\right\} \\ & \gtrsim c\epsilon_n/p. \end{aligned}$$

Noting that $1 - \exp\left\{\frac{c\epsilon_n/p-\omega_{0,ij}}{2v_{g_{ij}}}\right\} - \exp\left\{\frac{-c\epsilon_n/p-\omega_{0,ij}}{2v_{g_{ij}}}\right\}$ is positive when $\epsilon_n = 0$ under the conditions for $v_{g_{ij}}$ is sufficient to obtain the limit result.

Focusing now on the term referring to diagonal elements of Ω , we have that

$$\begin{aligned} & \int_{c\epsilon_n/p-\omega_{0,ii}}^{c\epsilon_n/p+\omega_{0,ii}} \frac{\theta}{2} e^{-\frac{\theta}{2}\omega_{ii}} d\omega_{ii} = \exp\left\{-\frac{\theta}{2}(c\epsilon_n/p - \omega_{0,ii})\right\} \\ & \quad - \exp\left\{-\frac{\theta}{2}(c\epsilon_n/p + \omega_{0,ii})\right\}. \end{aligned}$$

Using the same argument as above, we can show

$$\int_{c\epsilon_n/p-\omega_{0,ii}}^{c\epsilon_n/p+\omega_{0,ii}} \frac{\theta}{2} e^{-\frac{\theta}{2}\omega_{ii}} d\omega_{ii} \gtrsim c\epsilon_n/p,$$

since the limit of the same ratio as previous term for ϵ_n to 0 converges to zero. These two results complete the proof. \square

Using the prior concentration result stated in Proposition 2, we can investigate the posterior convergence rate of the graphical parameters. Proposition 3 shows how the posterior convergence rate of our model is equal to the convergence rate of the graphical lasso (Friedman et al., 2008) and the Bayesian graphical lasso (Park and Casella, 2008). Note that, in Proposition 3, the prior distribution for the precision matrix in Equation (19) is slightly different from the one used in our model in Equation (11) since it includes the probability $P(\bar{R} \geq |\mathbf{G}|)$ to penalize denser graphs. However, in the context of MCMC algorithm to sample from posterior distribution, such probability has little to no effect. The ratio of this probabilities is, indeed, close or superior to 1 for most proposal distributions.

Proposition 3. Let $X^{(n)} = (X_1, \dots, X_n)$ be a random sample from the p -dimensional Gaussian distribution with mean 0 and precision matrix $\Omega_0 \in \mathcal{U}(\epsilon_0, l) = \{\Omega : |\{(i, j) : 1 \leq i < j \leq p, \omega_{ij} \neq 0\}| \leq l, 0 < \epsilon_0 \leq \text{eig}(\Omega)_1 < \text{eig}(\Omega)_p \leq \epsilon_0^{-1} < \infty\}$ for some $0 < \epsilon_0 < \infty$ and $0 \leq l \leq p(1-p)/2$. Also assume that the prior distributions are:

$$p(\boldsymbol{\Omega} \mid \mathbf{G}, v_0, v_1, \theta) = \frac{1}{K(\mathbf{G}, v_0, v_1, \theta)} \prod_{j < j'} N(\omega_{jj'} \mid 0, v_{g_{jj'}}) \prod_j \text{Exp}(\omega_{jj} \mid \theta/2)$$

with $v_{g_{ij}} \leq \frac{\|\Omega_0\|_\infty}{2 \log 2}$ and

$$p(\mathbf{G} \mid v_0, v_1, \theta, \xi) = \frac{K(\mathbf{G}, v_0, v_1, \theta)}{K(v_0, v_1, \xi)} \prod_{j < j'} \xi^{g_{jj'}} (1 - \xi)^{1 - g_{jj'}} P(\bar{R} \geq |\mathbf{G}|), \quad (19)$$

with $\xi < 0.5$ and $P(\bar{R} > a_1 m) \leq \exp\{-a_2 m \log m\}$ for some constants a_1 and a_2 and $m = 1, 2, \dots$. Then,

$$\mathbb{E}_0[P\{\|\Omega - \Omega_0\|_2 > M\epsilon_n \mid X^{(n)}\}] \rightarrow 0$$

for $\epsilon_n = n^{-1/2}(p+l)^{1/2}(\log p)^{1/2}$ and sufficiently large constant M .

Proof. Similarly to Banerjee and Ghosal (2015), this proof uses the general theory of posterior convergence rate developed in Ghosal et al. (2000). First, we need to prove that the prior probability assigns enough mass to the Kullback-Leibler neighborhood of the true value. Then we show that the space in which the true parameter is contained is not too big in terms of metric entropy with respect to the Frobenius distance. Finally, we prove that the prior probability for matrices not contained in the the same space of the true value is not too high.

More in detail, Proposition 2 shows that

$$\Pi(B(p_{\Omega_0}, \epsilon_n)) \gtrsim (c\epsilon_n/p)^{p+l}$$

where $B(p_{\Omega_0}, \epsilon_n) = \{p : K(p_{\Omega_0}, p_\Omega) \leq \epsilon_n^2, V(p_{\Omega_0}, p_\Omega) \leq \epsilon_n^2\}$ with $K(f, g) = \int f \log(f/g)$ and $V(f, g) = \int f \log^2(f/g)$. By Theorem 2.1 of Ghosal et al. (2000), this implies

$$(p+l)(\log p + \log \epsilon_n^{-1}) \asymp n\epsilon_n^2$$

so as to get $\epsilon_n = n^{-1/2}(p+l)^{1/2}(\log p)^{1/2}$ as the prior concentration rate around Ω_0 . Using the same argument of Theorem 3.1 in Banerjee and Ghosal (2015), we can show that the metric entropy of a subset of \mathcal{U} is bounded. In particular, consider the set \mathcal{P}_n to be the space of all densities p_Ω such that the graph induced by Ω has maximum number of edges $\bar{r} < p(p-1)/4$ and each entry of Ω is at most L in absolute value, where \bar{r} and L depend on n and are to be chosen later. Then, the metric entropy of the set of precision matrices with respect to the Frobenius distance is given by

$$\begin{aligned} \log \left\{ \sum_{j=1}^{\bar{r}} \left(\frac{L}{\epsilon_n} \right)^j \binom{\binom{p}{2}}{j} \right\} &\leq \log \left\{ \bar{r} \left(\frac{L}{\epsilon_n} \right)^{\bar{r}} \binom{p + \binom{p}{2}}{\bar{r}} \right\} \\ &\lesssim \log \bar{r} + \bar{r} \log L + \bar{r} \log \epsilon_n^{-1} + \bar{r} \log p, \end{aligned}$$

so the choices $\bar{r} \sim b_1 n \epsilon_n^2 / \log n$, and $L \sim b_2 n \epsilon_n^2$ for any choice of the constants b_1 and $b_2 > 0$ will satisfy the rate equation

$$\log \bar{r} + \bar{r} \log p + \bar{r} \log \epsilon_n^{-1} + \bar{r} \log(n \epsilon_n^2) \asymp n \epsilon_n^2.$$

Note that, under condition $n \epsilon_n^2 / \log n \ll p(p-1)/2$, the requirement $\bar{r} < p(p-1)/4$ is satisfied as $n \rightarrow \infty$.

Finally, we need to bound the prior probability of the complementary set \mathcal{P}_n^c . Note that a distribution p_Ω can be outside of \mathcal{P}_n only if the graph induced by Ω has more edges than \bar{r} or if any entry of the matrix Ω has larger magnitude than L . The probability of the second event is bounded by $p(1-p)/2 e^{-L^2}$ which, by the choice of $L \sim b_2 n \epsilon_n^2$, is bounded by $\exp\{-b_3 n \epsilon_n\}$ for some constant b_3 . Since b_2 can be taken as large as we want, b_3 can also be taken as large as required. The prior probability of having more than \bar{r} edges is

$$P(\bar{R} > \bar{r}) \leq \exp(-a'_2 b_1 n \epsilon_n^2),$$

where $a'_2 b_1$ can be made as large as possible by making b_1 large. Hence $\epsilon_n = n^{-1/2}(p+l)^{1/2}(\log p)^{1/2}$ is the posterior convergence rate. \square

Proposition 3 shows that, with sufficiently small prior variances, the posterior mean of

the precision matrix Ω converges to the true one with the same rate as the convergence rate of graphical lasso (Rothman et al., 2008). Therefore, employing similar arguments as in Barber et al. (2020), for a sufficiently large sample size, our model controls the frequentist FDR and, consequently, the expected BFDR under a threshold q without the knowledge of the true precision matrix Ω .

3 Simulation study

We evaluate the performance of the proposed model through a comprehensive simulation study and compare results with those of the classical model-X knockoff filter and state-of-the-art variable selection methods, including lasso regression (Tibshirani, 1996) and models that use discrete spike-and-slab priors (Mitchell and Beauchamp, 1988).

3.1 Data generation

We generated data from a few distinct scenarios. In Scenario 1, we generated $p = 30$ covariates independently sampled from a standard Gaussian distribution. Out of the 30 covariates, we assumed that 6 of them have a linear effect on the response variable y . The regression coefficients associated with these active covariates were randomly selected from the set $\{\pm 0.5, \pm 1, \pm 1.5\}$ to introduce variation in the strength of the effects. We then simulated the response variable from the linear equation $y_i = x_i\beta + \epsilon_i$, with $\epsilon_i \sim N(0, \sigma_\epsilon)$ and $\sigma_\epsilon = 1$, for $i = 1, \dots, n$. This relatively simple scenario enables us to assess the capability of our model to recover the set of active variables when the graphical structure learning is, effectively, a source of noise in the model. In Scenario 2, we introduce a more realistic setting by incorporating a correlation structure among the predictors. More specifically, the 30 covariates were generated from a Gaussian graphical model, where the underlying graph structure is characterized by a sparse precision matrix. The underlying graph structure is shown in Figure 1. Similarly to Scenario 1, we selected 6 out of the 30 variables to be active in explaining the response y and randomly sampled their coefficient values from the set $\{\pm 0.5, \pm 1\}$. In Scenario 3, data are simulated following the setting of Li and Li (2008) and Peterson et al. (2016). Specifically, we generated the covariates from a graph with 40

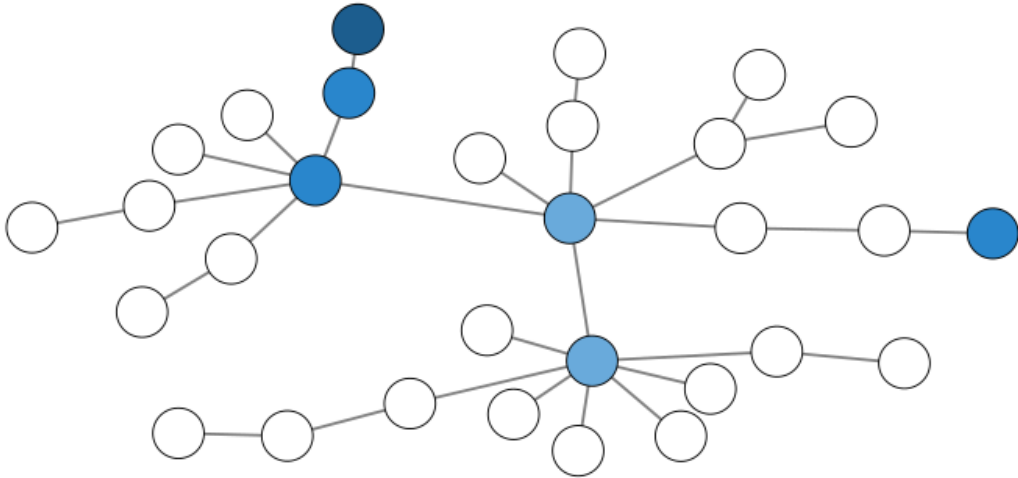


Figure 1: **Simulation study:** Scale-free graph structure under Gaussian graphical model in Scenario 2. White nodes correspond to the noise variables, and blue nodes to the active ones. A stronger blue color corresponds to a larger effect.

hubs, each with 5 connected nodes. This resulted in 240 covariates with a sparse graphical model of 200 edges in total. We set as active variables those in the first 4 hubs, plus their connected edges, resulting in a total of 24 non-zero coefficients. In particular the regression coefficients of the 4 hubs are 5, -5 , 3 and -3 , respectively, while the coefficients of the associated nodes are the same but divided by $\sqrt{10}$. The covariates were then generated from a Gaussian distribution with zero mean and covariance matrix Σ with diagonal elements equal to 1 and covariances between connected variables equal to 0.7. As in the previous scenarios, the response variable was simulated from a linear Gaussian model with the error variance equal to $\sum_j \beta_j^2/4$. In each scenario we set the sample size at $n = 200$ and considered 100 replicated data sets.

3.2 Parameter settings

When fitting our model, we need to specify the hyperparameters of the shrinkage inducing prior (10) on the precision matrix of the covariates' graph, the spike-and-slab priors (12) on the regression coefficients and the Ising prior (13) on the selection indicators. In all analyses, for prior (10) on the precision matrix, following the recommendations in Wang (2015), we used $v_0 = 0.01^2$ and $v_1 = hv_0$ with $h = 100$. We set the prior probability of edge selection ξ

to 0.01 and the exponential parameter θ for the elements on the diagonal to 2. To specify vaguely informative priors, we set $h_\beta = 1$ in the joint prior (12) on the regression coefficients, and $\alpha_\sigma = \beta_\sigma = 2$ for the prior (14) on the error variance. Furthermore, we centered covariates and response variables, ensuring that the intercept term in the model is zero. Smith (1973) showed that, in the Bayesian framework, setting the intercept term to zero is equivalent to placing a Gaussian prior with infinite variance on the intercept parameter. Finally, for the Ising prior (13) on γ , we set $a = b = 0.5$. This specification corresponds to a prior inclusion probability of 0.622 on the original variable or its knockoff, when the graph is empty. When experimenting with this prior, we found non-sparse specifications to work well, as the Bayesian knockoff framework allows for further control of the FDR by excluding inactive covariates. We provide sensitivity analyses to these prior choices in Section 3.5.

When initializing the MCMC algorithm, we set the selection indicators γ to 0 and assumed independent covariates with $\mathbf{\Omega} = \mathbf{I}$. The results reported below in Section 3.3 are obtained by running MCMC chains with 8,000 iterations for burn-in, followed by 8,000 iterations for inference. For each chain, we assessed convergence by using the Geweke’s diagnostic test (Geweke, 1992) to check for signs of non-convergence. For example, the average z -scores from the test for $\{(\beta_j, \tilde{\beta}_j)\}_{j=1}^p$ were 0.03, 0.01 and -0.05 for Scenario 1, Scenario 2 and Scenario 3, respectively. This suggests that the algorithm has run for enough iterations.

3.3 Results and comparisons

Let us first examine a single data set to gain insight into how the proposed model works. Specifically, we focus on a randomly selected data set generated under Scenario 2. Figure 2 shows the posterior distribution of the feature statistics W_j , $j = 1, \dots, p$, and Figure 3 shows the behavior of the proposed Bayesian knockoffs on this simulated data set. Bars in this plot correspond to quantities $\hat{\mathbb{P}}[r_j = 0 \mid \mathbf{D}]$, $j = 1, \dots, p$, calculated as in Equation (18), while points represent the estimated $\text{BFDR}(\mathcal{S})$ with \mathcal{S} the set of all previous indexes. The dashed red line indicates the chosen threshold $q = 0.1$. Points in red correspond to the true active variables and those in green to the inactive ones. The final set of selected variables is $X_{\mathcal{S}} = \{X_1, X_2, X_6, X_{24}, X_{30}\}$ and it contains exactly the true active variables, showing that the model can effectively distinguish between active and inactive variables.

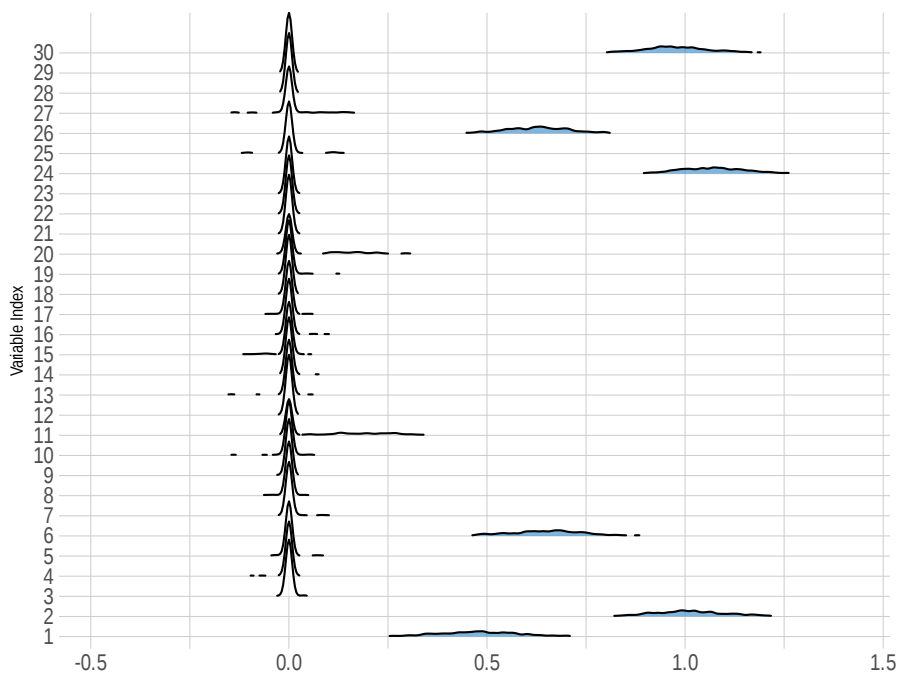


Figure 2: **Simulation study:** Posterior distribution of W_j , $j = 1, \dots, p$, for a simulated data set under Scenario 2. Those highlighted in blue are selected according to Figure 3.

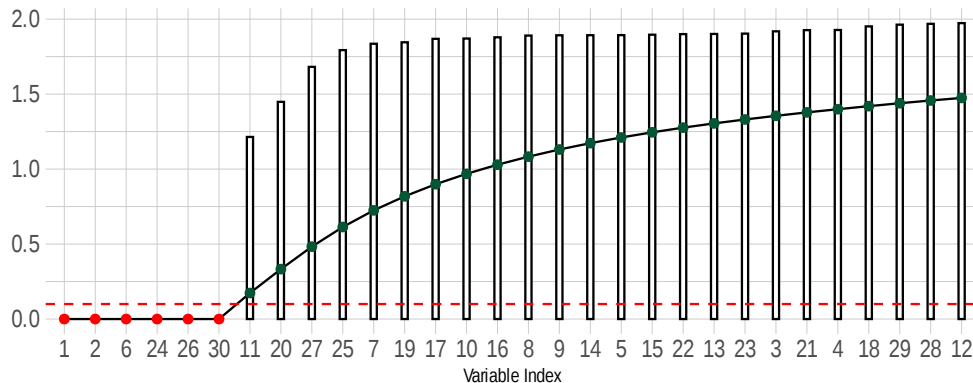


Figure 3: **Simulation study:** Behavior of the proposed method for variable selection for a simulated data set under Scenario 2. Bars represent estimates $\widehat{\mathbb{P}}[r_j = 0 \mid \mathbf{D}]$, $j = 1, \dots, p$, in increasing order and points represent the estimated BFDR(\mathcal{S}) with \mathcal{S} the set of all previous indexes. The dashed red line is the chosen threshold $q = 0.1$. Points in red correspond to true active variables and those in green to inactive variables.

Next, we report the comparison of the performances of our proposed model with other procedures for variable selection with and without FDR control. Among these procedures, we include the classical model-X knockoff filter proposed by Barber and Candès (2019). In particular, we consider two versions of model-X knockoff filter, one with the true covariance matrix assumed known, and one with an estimate of Σ obtained via the graphical lasso estimator of Friedman et al. (2008). Indeed, Barber et al. (2020) proved that, under certain conditions, the graphical lasso can be used to preserve the FDR guarantees of knockoff filters. For both our model and the classical knockoff filter, we fix the FDR threshold at $q = 0.1$. The knockoffs were generated using the R package `knockoffs`, and the covariance matrix was estimated using the `glasso` package. In addition to the model-X knockoff filter, our comparison includes other state-of-art methods for variable selection. In particular, we include the Lasso regression (Tibshirani, 1996) and a Bayesian linear regression model with discrete spike-and-slab prior and a Beta hyperprior on the inclusion probability. We also considered the joint edge and regression estimation model proposed by Peterson et al. (2016), which we implemented ourselves as a version of our proposed model without knockoffs latent

variables. The regularizing parameter for lasso regression was determined by minimizing the cross-validated error using the R package `glmnet`. We note that this method does not employ any FDR correction. Variable selection for the Bayesian and joint estimation methods was achieved by thresholding the marginal posterior probabilities of inclusion (PPIs) at 0.5, following the median model approach (Barbieri and Berger, 2004). We also considered the BFDR approach proposed by Newton et al. (2004).

To compare performance, in Table 1 we report averages and standard deviations across 100 replicates of several evaluation metrics. In particular, we consider FDR, True Positive Rate (TPR), Matthew Correlation Coefficient (MCC), and F1-score. Let TP be the number of true positives, TN the number of true negatives, FP the number of false positives, and FN the number of false negatives. We can then define the performance metrics used as

$$\begin{aligned}
 FDR &= \frac{FP}{FP + TP}, & TPR &= \frac{TP}{TP + FN}, \\
 MCC &= \frac{TP \times TN - FP \times FN}{\sqrt{(TP + FP)(TP + FN)(TN + FP)(TN + FN)}}, \\
 F1 &= \frac{2 \times TP}{2 \times TP + FP + FN}.
 \end{aligned}$$

Results in Table 1 indicate that the proposed Bayesian method succeeds in keeping the FDR below the given threshold in every scenario, while achieving strong performances in TPR compared to the other methods, as well as MCC and F1 scores. It is worth noting that the classical knockoff filter exhibits low TPR in Scenarios 1 and 2, where the magnitude of the true coefficients is rather small. In other settings, not reported here, where the signal was strong and the sample size larger, we noticed improved performances for all methods, including classical knockoffs. Further, the values of the standard deviations for the TPR of the knockoff filter in the first two scenarios are higher than those of the other methods. This happens because, across the 100 simulated data sets, the knockoff filter TPR is often zero and sometimes quite high. Finally, we note that classical knockoff has a slightly higher FDR than the threshold 0.1 when the covariates are not independent and the covariance matrix is estimated using graphical lasso. As shown in Barber et al. (2020), the classical knockoff filter does not control FDR exactly below q when the covariance matrix used to

build the knockoffs is not the true one but an estimate. In our case, the graphical lasso tends to produce a sparser than needed graph. This behavior also supports our choice of setting the parameter of the priors in the proposed method to obtain a generally dense graph to be used to generate the knockoffs. Results for the third scenario confirm that the proposed Bayesian Knockoff filter is also able to outperform the state-of-art methods in settings with larger dimensionality. As a matter of fact, it successfully controls FDR under 0.1, unlike the lasso regression. Moreover, the TPR is on average comparable to the one of the classical knockoff filter but it is more stable as it has a much lower standard deviation.

As for the comparison with the state-of-art methods for variable selection, we can see that Lasso has a high TPR in every scenario but also a high FDR. Indeed, Meinshausen and Bühlmann (2006) noted that the lasso estimator tends to include too many inactive predictors when the penalization parameter is chosen to have low prediction error, as we did in our simulations. Compared with Bayesian variable selection via spike-and-slab prior, our model offers comparable results in the first two scenarios, where the covariates are independent, with almost perfect results. In the third scenario, with dependent covariates, spike-and-slab loses the control of FDR, unlike our method, even though it manages to find more relevant predictors than our method. In Table 1 we do not show results for the BFDR approach proposed by Newton et al. (2004). Indeed, BFDR selected exactly the same variables as spike-and-slab in the first two scenarios. In the third scenario, however, the PPIs were hovering around 0.5 and the BFDR did not select any variable. As pointed out in the introduction section, Bayes FDR selection procedures rely on the estimates of the marginal PPIs, as obtained from the MCMC output, while our procedure employs an upper bound on the probabilities of non-inclusion. Therefore, our model appears to achieve good operating characteristics and to control the FDR even when the estimates of the marginal posterior probability of inclusion fail to select the true relevant variables. This is evident when comparing our method with the model proposed by Peterson et al. (2016) (Joint). In scenarios 1 and 2 the two methods have the same performances, while in scenario 3, even though MCC and F1 have similar values, the addition of the knockoffs allows to keep the FDR under the desired level, while the joint method has higher FDR and therefore not an explicit control over it.

Table 1: **Simulation study:** FDR, TPR, MCC and F1-score, for the scenarios described in Section 3.1. Compared methods are the proposed model (BayesKnock) classical Knockoff filter with exact (Knockoff (Exact)) and estimated (Knockoff (Glasso)) covariance matrix, Lasso, spike-and-slab regression (Spike-Slab) and the joint model proposed by Peterson et al. (2016) (Joint). Values reported are averages over 100 replicated data sets, with standard deviations in parentheses.

		Scenario 1	Scenario 2	Scenario 3
FDR	BayesKnock	0.007 (0.03)	0.013 (0.05)	0.032 (0.05)
	Knockoff (Exact)	0.035 (0.11)	0.025 (0.09)	0.055 (0.08)
	Knockoff (Glasso)	0.070 (0.16)	0.114 (0.19)	0.079 (0.08)
	Lasso	0.543 (0.14)	0.557 (0.12)	0.437 (0.12)
	Spike-Slab	0.000 (0.00)	0.003 (0.02)	0.716 (0.04)
	Joint	0.029 (0.06)	0.043 (0.07)	0.177 (0.11)
TPR	BayesKnock	1.000 (0.00)	0.977 (0.07)	0.560 (0.10)
	Knockoff (Exact)	0.088 (0.28)	0.068 (0.25)	0.592 (0.36)
	Knockoff (Glasso)	0.162 (0.37)	0.277 (0.45)	0.595 (0.39)
	Lasso	1.000 (0.00)	1.000 (0.00)	0.934 (0.05)
	Spike-Slab	0.999 (0.01)	0.979 (0.06)	0.820 (0.06)
	Joint	1.000 (0.00)	1.000 (0.00)	0.664 (0.08)
MCC	BayesKnock	0.995 (0.02)	0.973 (0.06)	0.714 (0.07)
	Knockoff (Exact)	0.065 (0.21)	0.059 (0.20)	0.627 (0.37)
	Knockoff (Glasso)	0.109 (0.25)	0.188 (0.31)	0.612 (0.41)
	Lasso	0.544 (0.15)	0.536 (0.14)	0.682 (0.09)
	Spike-Slab	0.999 (0.01)	0.986 (0.05)	0.389 (0.05)
	Joint	0.981 (0.04)	0.972 (0.05)	0.711 (0.08)
F1	BayesKnock	0.996 (0.02)	0.977 (0.06)	0.704 (0.08)
	Knockoff (Exact)	0.069 (0.22)	0.062 (0.21)	0.631 (0.37)
	Knockoff (Glasso)	0.117 (0.27)	0.201 (0.33)	0.629 (0.38)
	Lasso	0.614 (0.12)	0.608 (0.11)	0.693 (0.09)
	Spike-Slab	0.999 (0.01)	0.988 (0.04)	0.420 (0.04)
	Joint	0.985 (0.03)	0.977 (0.04)	0.729 (0.07)

We note that, with our proposed method, posterior inference results not only in variable selection but also in learning the underlying graph structure among the covariates via the inference on the precision matrix $\mathbf{\Omega}$. For example, the median graph can be obtained by thresholding the marginal posterior probability of inclusion (PPI) of edge inclusion at 0.5. This approach of using a threshold for PPIs is commonly employed in graph structural learning tasks as the space of possible graphs is too big to be explored entirely, making it impossible to select the most frequently encountered graph. When looking at the Frobenius norm of the difference between the posterior mean of $\mathbf{\Omega}$ and the true precision matrix,

$$\|\mathbf{\Omega} - \widehat{\mathbf{\Omega}}\|_F = \sqrt{\sum_{i,j} (\omega_{ij} - \hat{\omega}_{ij})^2},$$

our model achieved very solid performances for graph selection across the scenarios. For example, the average Frobenius norm was 1.404, 1.415 and 9.425 and the F1-score was 0.869, 0.865 and 0.99 in Scenarios 1, 2 and 3, respectively. Note that the Frobenius norm is much higher in Scenario 3 due to the different magnitude in the correlation between variables. However, as we can see from the F1-score, the graph recovery still works.

3.4 Accelerated Failure Time models

We also show a simulation for a regression model with a survival outcome, specifically an accelerated failure time (AFT) model, with censored observations. To use the proposed Bayesian knockoff filter, we adapt the stochastic search MCMC procedure of Sha et al. (2006), that makes use of data augmentation techniques (Tanner and Wong, 1987). Let T_i represent the time-to-event for the i -th subject and c_i the censoring time. AFT models assume a multiplicative effect on the survival times of the general form $\log(T_i) = X_i\beta + \epsilon_i$, where the errors ϵ_i may have several distributions. Here, we assume the errors to be i.i.d. Gaussian variables. To allow for censored observations, we introduce a latent variable y_i such that

$$\begin{cases} y_i = \log(T_i^*) & \text{if } \kappa_i = 1 \\ y_i > \log(T_i^*) & \text{if } \kappa_i = 0 \end{cases}.$$

Table 2: **Simulation study:** FDR, TPR, MCC and F1-score, for the AFT models. Compared methods are the proposed model (BayesKnock), spike-and-slab regression (Spike-Slab) and the joint model proposed by Peterson et al. (2016) (Joint). Values reported are averages over 100 replicated data sets, with standard deviations in parentheses.

	FDR	TPR	MCC	F1
BayesKnock	0.035 (0.03)	0.526 (0.11)	0.713 (0.08)	0.701 (0.10)
Spike-Slab	0.642 (0.04)	0.742 (0.01)	0.239 (0.08)	0.311 (0.08)
Joint	0.192 (0.13)	0.592 (0.04)	0.701 (0.09)	0.712 (0.10)

where T_i^* is defined as $\min(T_i, c_i)$ and $\kappa_i = \mathbb{1}_{T_i \leq c_i}$ is the censoring indicator. Here, we assume that the latent variable y_i given the covariates X follows the model described in Equation (9) with $p(Y | X, U)$ as in Equation (8), with the same prior specification. We generate the covariates following the scheme employed in Scenario 3 above, and then generate the log of the survival times from the linear AFT model. We allow for 25 % of the subjects to be censored. Table 2 shows performances of our proposed method, compared to the spike-and-slab method for AFT models of Sha et al. (2004) and to the same AFT model without knockoff latent variable, as also implemented by Peterson et al. (2016). These results are consistent with those for Scenario 3 in the previous simulation and also show that the proposed procedure suffers the least from the presence of censored data.

3.5 Sensitivity analysis

Table 3 shows the results of the sensitivity analysis. We started from the same setting adopted in the simulation study for Scenario 2 and then varied one hyperparameter at a time. We found that posterior inference is robust to the choice of the hyperparameters, except for v_0 in the prior on the precision matrix $\mathbf{\Omega}$ in Equation (10). Both Wang (2015) and Peterson et al. (2016) report the same sensitivity. We notice, however, that the choice of v_0 does not affect the selection performances of our method. As noted in Barber et al. (2020), knockoffs can still be used with estimated distributions, but the control on FDR is affected by the Kullback-Leiber distance between the estimate and the true distribution. As a matter of fact, in Gaussian graphical models, imposing too many zeros strongly affects the estimates of the non-zero off-diagonal elements on the precision matrix $\mathbf{\Omega}$. For this reason,

Table 3: **Simulation study:** Sensitivity analysis.

Hyperparameter	FDR	TPR	Frobenius Loss	F1 Score
$a = -2.5$	0.000	1.000	1.624	0.800
$a = -0.5$	0.000	1.000	1.617	0.840
$a = 0.5$	0.000	1.000	1.607	0.824
$a = 2.5$	0.142	1.000	1.662	0.800
$b = -2.5$	0.000	0.833	1.625	0.816
$b = -0.5$	0.000	0.833	1.600	0.840
$b = 0.5$	0.000	1.000	1.607	0.824
$b = 2.5$	0.333	1.000	1.645	0.816
$v_0 = 0.01^2$	0.000	1.000	1.620	0.816
$v_0 = 0.1^2$	0.000	1.000	2.435	0.067
$v_0 = 0.5^2$	0.000	1.000	4.134	0.000
$v_1 = 0.25$	0.000	1.000	1.525	0.840
$v_1 = 1.00$	0.000	1.000	1.645	0.816
$v_1 = 25.00$	0.000	1.000	1.708	0.840
$v_1 = 100.00$	0.000	1.000	1.901	0.766

we recommend setting the hyperparameters v_0 and v_1 to obtain a slightly denser graph.

4 Application to prostate cancer data

As an illustrative example, we examine a data set on prostate cancer obtained from Stamey et al. (1989) and widely used as a benchmark data set (see, for instance, Tibshirani, 1996; Zou and Hastie, 2005, among others). The aim is to investigate the association between Prostate-Specific Antigen (PSA) levels and various clinical measures in a sample of 97 men, who were preparing to undergo radical prostatectomy. PSA is a protein produced by normal and malignant prostate cells and is useful as a preoperative marker as prostate cancer releases PSA into the bloodstream. Additionally, eight clinical measures are included: the logarithm of the cancer volume (in cm^3) (`lcavol`), the logarithm of the prostate weight (in g) (`lweight`), patient age (`age`), the logarithm of the bad prostatic hyperplasia (in cm^2) (`lbph`), the logarithm of capsular penetration (in cm) (`lcp`), seminal vesicle invasion (`svi`), the current Gleason score (`gleason`) and the percentage of Gleason scores four or five out of five (`pgg45`). The logarithm of the PSA (ng/ml) is the response variable. The presence of seminal vesicle invasion is a binary variable (1 = yes, 0 = no) and `gleason` is a discrete nu-

merical variable with four values. The Gleason score relates to the current grade of prostate cancer, while the predictor `pgg45` provides information about the patient’s history of the Gleason scores, and it is strongly linked to the current final score Gleason score.

For our analysis, we considered the subset of 73 subjects without seminal vesicle invasion and with no severe cancer (Gleason score less than 9). To ensure the appropriate statistical assumptions, we applied the nonparanormal transformation (Liu et al., 2009) to the covariates. This transformation provides a Gaussian marginal distribution of each covariate and assumes a Gaussian copula on their joint distribution. We tested the joint Gaussian assumption after this transformation using the multivariate Shapiro test (Villasenor Alva and Estrada, 2009), obtaining a p -value of 0.02. In our application, we used the same hyperparameter settings as in the simulation study, and ran an MCMC chain with 8,000 iteration for burn-in followed by 8,000 iterations for inference. The average z -scores from the Geweke’s test for $\{(\beta_j, \tilde{\beta}_j)\}_{j=1}^p$ was -0.22 .

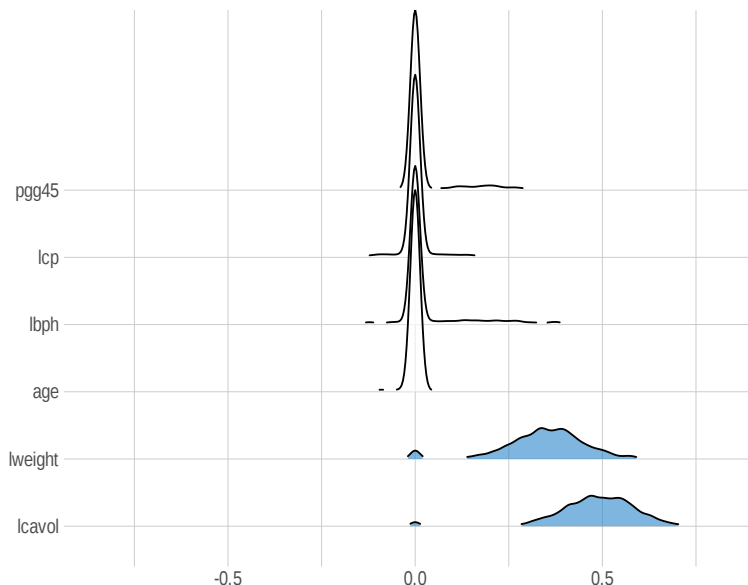


Figure 4: **Prostate cancer data:** Posterior distribution of W_j , $j = 1, \dots, 6$. Those highlighted in blue are selected according to Figure 5

Figure 4 shows the posterior distribution of the feature statistics W_j , $j = 1, \dots, p$ for each covariate in the model, with the selected variables shown in blue. Notably, the posterior distribution of the non-selected variables is symmetric around zero, while the selected variables exhibit a positive-centered distribution. Additionally, Figure 5 reports the estimated values

of $2\widehat{\mathbb{P}}[W_j \leq 0 \mid \mathbf{D}]$, $j = 1, \dots, 6$, in increasing order, together with the corresponding estimated $\text{BFDR}(\mathcal{S})$. Therefore, setting $q = 0.1$, the covariates to be selected are the logarithm of cancer volume and the logarithm of prostate weight.

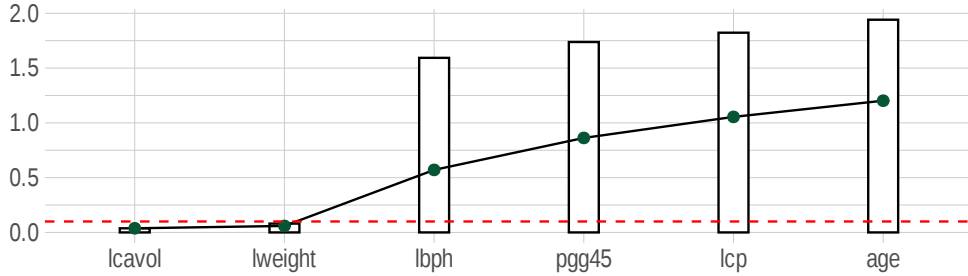


Figure 5: **Prostate cancer data:** Variable selection. Bars represent estimates $2\widehat{\mathbb{P}}[W_j \leq 0 \mid \mathbf{D}]$, $j = 1, \dots, 6$, in increasing order and points represent the estimated $\text{BFDR}(\mathcal{S})$ with \mathcal{S} the set of all previous indexes. The dashed red line is the chosen threshold $q = 0.1$.

We also applied the state-of-art procedures used for comparison in the simulation study. Table 4 summarizes the results. We can see that classical knockoff filter does not find any association between covariates and PSA production level. Spike-and-slab regression selects the same covariates as the proposed method, and the joint estimation model selects one additional variable. Lasso, as we saw in the simulation study, selects many variables, including the two selected by our method. We acknowledge that the Bayesian procedures are computationally more expensive than the classical methods. For example, running the MCMC for our proposed method on this application took 35 minutes on a regular laptop equipped with Intel(R) Core(TM) i7-9750H CPU @ 2.60GHz. However, relying on a posterior distribution of the knockoff variables increases stability of the selection, as our simulations have shown.

5 Concluding remarks

In this article, we have proposed an approach that generalizes the model-X knockoff filter of Candès et al. (2018) to the Bayesian framework. Our formulation allows for variable selection while controlling the BFDR at an arbitrary level, making use of knockoffs as latent

Table 4: **Prostate cancer data:** Selection of variables using different variable selection methods.

Variable	BayesKnock	Knockoff Filter	Lasso	Spike-and-slab	Joint
lcavol	✓	-	✓	✓	✓
lweight	✓	-	✓	✓	✓
age	-	-	-	-	-
lbph	-	-	✓	-	✓
lcp	-	-	-	-	-
pgg45	-	-	✓	-	-

variables that act as negative controls. Additionally, we have imposed a sparse conditional independence structure on the covariates and used it in the prior on the knockoffs in a way that satisfies their pairwise conditional independence property. We have also limited the computational cost by adopting a modified version of the spike-and-slab prior that avoids the increase of the model dimension. Our model performs variable selection using an upper bound on the posterior probability of non-inclusion. We have shown how our model construction leads to valid model-X knockoffs and demonstrated that the proposed approach is sufficient for controlling the BFDR at an arbitrary level, in finite samples. We have also shown that the model selection is robust to the estimation of the precision matrix.

In applications, we have shown that our proposal increases the stability of the selection, since it relies on the entire posterior distribution of the knockoff variables instead of a single sample. Results from our simulation study have shown how in simple settings (like Scenarios 1 and 2) our Bayesian knockoff filter approach has similar performance to state-of-art Bayesian variable selection techniques, such as spike-and-slab priors, while outperforming classical variable selection methods, including classical knockoffs filter. Moreover, under more complex dependence structure of the covariates (as in Scenario 3), our proposal is able to control the FDR under any desired threshold, unlike spike-and-slab variable selection methods, that suffer from poor estimates of the PPIs. It also performs as well as classical knockoff filter with covariance structure known. This is relevant since in practice the precision matrix is never known. As an illustrative example, we have applied the model to a benchmark data set on prostate cancer collected from the study of Stamey et al. (1989), and found more relevant variables than the classical knockoff filter.

Future work could extend this research in several directions. First, while we have assumed a standard Gaussian linear regression setting, similar Bayesian knockoff filters could be designed for linear settings that incorporate discrete-type responses. For example, in the simulations we have also considered an AFT model for survival outcomes. A similar extension, that uses data augmentation techniques, can be used for multinomial probit models (Albert and Chib, 1993; Sha et al., 2004). Furthermore, logit and negative binomial responses could be accommodated via the use of Polya-Gamma data augmentation schemes (Polson et al., 2013; Zhou et al., 2012). Another interesting direction would be to extend the proposed knockoffs framework to the case of non-Gaussian covariates. The generation of knockoffs for non Gaussian random variables is still an open research problem. This case presents the main challenge of not having a known distribution that respects pairwise exchangeability (Bates et al., 2021). A promising direction is represented by the approach proposed by Dreassi et al. (2024), which makes use of conditional independence to build the knockoffs variables. Finally, the variable selection prior distribution we have used on the coefficients presents some computational difficulties due to the need to use a Metropolis-within-Gibbs algorithm. As an alternative, a shrinkage prior such as the horseshoe prior (Carvalho et al., 2010), could be used to reduce computational costs. However, this reduced computational cost comes at the expense of greater difficulty in utilizing the information from the estimated graph on the covariates.

A Complete proof of Proposition 1

Theorem A.1. *Given the model in Equation (9), let $p(\beta, \tilde{\beta})$ be a prior distribution such that*

$$p(\beta, \tilde{\beta})_{\text{Swap}(j)} = p(\beta, \tilde{\beta}) \quad j = 1, \dots, p$$

and let $W = (W_1, \dots, W_p)^T$ be an anti-symmetric function of β and $\tilde{\beta}$. Let $r = (r_1, \dots, r_p) \in \{0, 1\}^p$ be a random vector such that $r_j = 0 \iff X_j \perp\!\!\!\perp Y \mid X_{-j}$. Then the posterior distribution of W obeys the sign-flip property, i.e.

$$\mathbb{P}[W_j > 0 \mid \mathbf{D}, r_j = 0] = \mathbb{P}[W_j < 0 \mid \mathbf{D}, r_j = 0]$$

Proof. In the context of this proof, the model in Equation (9) is equivalent to the simple linear model reported in Equation (7). The marginalization of latent knockoffs is, indeed, not required since for this proof both the conditional independence and the pairwise exchangeability properties are only required to be true a priori. Moreover, applying the knockoff decomposition in Equation (4) and working with their random part U is equivalent to work with the complete knockoffs \tilde{X} . Thus, we will rely on the complete knockoffs for simplicity. Therefore, this proof, which we report for completeness, follows from results in Gu and Yin (2021)

For all j such that $r_j = 0$, it holds that $X_j \perp\!\!\!\perp Y | X_{-j}$. Thus, we can write $X_{\mathcal{S}} \perp\!\!\!\perp Y | X_{-\mathcal{S}}$ where the set $\mathcal{S} = \{j \in \{1, \dots, p\} : r_j = 0\}$. Moreover, by prior conditional independence, we have

$$X_{\mathcal{S}} \perp\!\!\!\perp Y | X_{-\mathcal{S}}, \tilde{X}.$$

Since $p(X, \tilde{X})_{\text{swap}(j)} = p(X, \tilde{X})$, it is also true that $\tilde{X}_{\mathcal{S}} \perp\!\!\!\perp Y | \tilde{X}_{-\mathcal{S}}, X$. This implies

$$p(Y | X, \tilde{X}) = p(Y | X_{\text{swap}(\mathcal{S})}, \tilde{X}_{\text{swap}(\mathcal{S})}).$$

Equation (7) implies that the response variable and the augmented covariate matrix $[X, \tilde{X}]$ are related only through regression coefficient. So

$$p(Y | X_{\text{swap}(\mathcal{S})}, \tilde{X}_{\text{swap}(\mathcal{S})}; \beta, \tilde{\beta}, \sigma) = p(Y | X, \tilde{X}; \beta_{\text{swap}(\mathcal{S})}, \tilde{\beta}_{\text{swap}(\mathcal{S})}, \sigma).$$

Since the prior probability distribution of the coefficient is invariant to swaps, it holds that

$$p(\beta, \tilde{\beta} | \tilde{x}_1, \dots, \tilde{x}_n, \sigma, \mathbf{D}) = p(\beta_{\text{swap}(\mathcal{S})}, \tilde{\beta}_{\text{swap}(\mathcal{S})} | \tilde{x}_1, \dots, \tilde{x}_n, \sigma, \mathbf{D}).$$

We can, then, write the marginal posterior distribution of the coefficients as

$$\begin{aligned}
p(\beta, \tilde{\beta} | \mathbf{D}) &= \int p(\beta, \tilde{\beta} | \tilde{x}_1, \dots, \tilde{x}_n, \sigma, \mathbf{D}) p(\tilde{x}_1, \dots, \tilde{x}_n, \sigma, \mathbf{D}) d\tilde{x}_1 \dots d\tilde{x}_n d\sigma \\
&= \int p(\beta_{\text{swap}(\mathcal{S})}, \tilde{\beta}_{\text{swap}(\mathcal{S})} | \tilde{x}_1, \dots, \tilde{x}_n, \sigma, \mathbf{D}) p(\tilde{x}_1, \dots, \tilde{x}_n, \sigma, \mathbf{D}) d\tilde{x}_1 \dots d\tilde{x}_n d\sigma \\
&= p(\beta_{\text{swap}(\mathcal{S})}, \tilde{\beta}_{\text{swap}(\mathcal{S})} | \mathbf{D}).
\end{aligned}$$

Define the vector $W_{\mathcal{S}} = (W_{1,\mathcal{S}}, \dots, W_{p,\mathcal{S}})$ as

$$W_{j,\mathcal{S}} = \begin{cases} W_j & r_j = 1 \\ -W_j & r_j = 0. \end{cases}$$

Finally, this implies the following

$$\begin{aligned}
p(W_{\mathcal{S}} | \mathbf{D}) &= \int_{\Lambda_{W_{\mathcal{S}}}} p(\beta_{\text{swap}(\mathcal{S})}, \tilde{\beta}_{\text{swap}(\mathcal{S})} | \mathbf{D}) d\beta_{\text{swap}(\mathcal{S})} d\tilde{\beta}_{\text{swap}(\mathcal{S})} \\
&= \int_{\Lambda_W} p(\beta, \tilde{\beta} | \mathbf{D}) d\beta d\tilde{\beta} \\
&= p(W | \mathbf{D})
\end{aligned}$$

where Λ_W is the subspace of values of the vector $(\beta, \tilde{\beta})$ that share the same value of W . Note that the second equality follows by the fact that W is an antisymmetric function. \square

B Detailed MCMC procedure

Here we provide further details on the MCMC procedure. Overall, our proposed algorithm can be summarized by the following steps:

- (a) **Update the set of variable selection parameters $(\delta, \tilde{\delta}, \gamma)$ and the regression coefficients $(\beta, \tilde{\beta})$.** Since the regression coefficients β and $\tilde{\beta}$ are necessary to the construction of the statistics W used for variable selection, we cannot integrate them out. Therefore, we propose a joint update of the parameters based upon randomly sampling one index $i \in \{1, \dots, p\}$ and changing the value of the variable inclusion indicator γ_i .

Once the proposed value γ^* is obtained, we assign values for the parameters δ and $\tilde{\delta}$. Specifically, if $\gamma_j^* = 0$ both δ_j^* and $\tilde{\delta}_j^*$ are set to zero. Otherwise, we randomly set δ_j^* or $\tilde{\delta}_j^*$ to 1. Finally, the proposed value for the regression coefficient is drawn from a Gaussian distribution with mean 0 and variance 0.5 times the corresponding proposed indicator δ_j^* and $\tilde{\delta}_j^*$ for β^* and $\tilde{\beta}^*$, respectively. Note that the moves induced by the proposal density $q(\gamma, \delta, \tilde{\delta}, \beta, \tilde{\beta})$ are symmetric therefore the proposal ratio is equal to 1 and the Metropolis-Hastings ratio depends only on the likelihood ratio and the ratio of the priors. We can write the likelihood ratio r_Y as

$$\begin{aligned} r_Y &= \frac{p(Y|X, U, \beta^*, \tilde{\beta}^*, \mathbf{\Omega}, \sigma^2)}{p(Y|X, U, \beta, \tilde{\beta}, \mathbf{\Omega}, \sigma^2)} \\ &= \exp \left\{ -\frac{1}{2\sigma^2} \left[(y - \mathbf{X}[\beta^* + (I - \mathbf{\Omega}\text{diag}(s))\tilde{\beta}^*] - U\tilde{\beta}^*)^T (y - \mathbf{X}[\beta^* + (I - \mathbf{\Omega}\text{diag}(s))\tilde{\beta}^*] - U\tilde{\beta}^*) \right. \right. \\ &\quad \left. \left. - (y - \mathbf{X}[\beta + (I - \mathbf{\Omega}\text{diag}(s))\tilde{\beta}] - U\tilde{\beta})^T (y - \mathbf{X}[\beta + (I - \mathbf{\Omega}\text{diag}(s))\tilde{\beta}] - U\tilde{\beta}) \right] \right\}. \end{aligned}$$

Thus, the acceptance ratio of the Metropolis-Hastings algorithm of step (a) is

$$\begin{aligned} r &= r_Y \times \frac{p(\beta^*, \tilde{\beta}^* | \gamma^*, \sigma^2, h_\beta) p(\delta^*, \tilde{\delta}^* | \gamma^*) p(\gamma^* | \mathbf{G}, a, b)}{p(\beta, \tilde{\beta} | \gamma, \sigma^2, h_\beta) p(\delta, \tilde{\delta} | \gamma) p(\gamma | \mathbf{G}, a, b)} \\ &= r_Y \times \exp\{a\mathbb{1}(\gamma^* - \gamma) + b(\gamma^* - \gamma)^T \mathbf{G}(\gamma^* + \gamma)\} \times r_\beta \times r_\delta, \end{aligned}$$

where

$$\begin{aligned} r_\delta &= \begin{cases} 0.5 & \text{if } \gamma_j^* = 1 \\ 2 & \text{if } \gamma_j^* = 0 \end{cases} \\ r_\beta &= \begin{cases} \frac{1}{2\pi h_\beta \sigma^2} \exp \left\{ -\frac{1}{2\sqrt{h_\beta} \sigma} \beta_j^{*2} \right\} & \text{if } \gamma_j^* = 1 \text{ and } \delta_j^* = 1 \\ \frac{1}{2\pi h_\beta \sigma^2} \exp \left\{ -\frac{1}{2\sqrt{h_\beta} \sigma} \tilde{\beta}_j^{*2} \right\} & \text{if } \gamma_j^* = 1 \text{ and } \tilde{\delta}_j^* = 1 \\ 2\pi h_\beta \sigma^2 \exp \left\{ \frac{1}{2\sqrt{h_\beta} \sigma} \beta_j^2 \right\} & \text{if } \gamma_j^* = 0 \text{ and } \delta_j = 1 \\ 2\pi h_\beta \sigma^2 \exp \left\{ \frac{1}{2\sqrt{h_\beta} \sigma} \tilde{\beta}_j^2 \right\} & \text{if } \gamma_j^* = 0 \text{ and } \tilde{\delta}_j = 1 \end{cases}. \end{aligned}$$

To improve the mixing of the algorithm, step (a) contains a within-model update where for each index i such that $\delta_i = 1$ and for each j such that $\tilde{\delta}_j = 1$, we propose a new value for the corresponding regression coefficient β_i and $\tilde{\beta}_j$. In this step, the proposal distribution $q(\beta)$ is a Gaussian distribution with mean the current value of β and variance 0.5. To simplify notation, we focus on the within-model update for β since it is exactly the same for $\tilde{\beta}$. The acceptance ratio for this step r_W is

$$r_W = r_Y \times \exp \left\{ -\frac{1}{2\sigma\sqrt{h_\beta}} \left(\beta_i^{*2} - \beta_i^2 \right) \right\}.$$

- (b) **Update the graph parameters ($\mathbf{G}, \mathbf{\Omega}$).** This is done by Gibbs sampling using the full conditional distributions via the efficient block-sampling algorithm proposed by Wang (2015). First, each column of the precision matrix $\mathbf{\Omega}$ is sampled from its full conditional distribution. To do so, consider the following change of variable $(\omega_{12}, \omega_{22}) \mapsto (k = \omega_{12}, l = \omega_{22} - \omega_{12}^T \mathbf{\Omega}_{11}^{-1} \omega_{12})$ where the precision matrix has been decomposed as

$$\mathbf{\Omega} = \begin{pmatrix} \mathbf{\Omega}_{11} & \omega_{12} \\ \omega_{12}^T & \omega_{22} \end{pmatrix}.$$

Then, Wang (2015) showed how the full conditional of k is a Gaussian distribution with mean $-\mathbf{C}s_{12}$ and covariance matrix \mathbf{C} where $\mathbf{C} = \{(s_{22} + \theta)\mathbf{\Omega}_{11}^{-1} + \text{diag}(1/v_{12})\}^{-1}$. The full conditional of l is, instead, a Gamma distribution with parameters $n/2 + 1$ and $(s_{22} + \theta)/2$. In the full conditional distributions, \mathbf{S} is the sample covariance matrix, and \mathbf{V} is a matrix with 0 on the diagonal and $v_{g_{jj'}}$ on the off-diagonal entries. Both of these matrices have been decomposed as $\mathbf{\Omega}$. Once the precision matrix $\mathbf{\Omega}$ has been updated, the full conditional distribution of the adjacency matrix is

$$\mathbb{P}(g_{i,j} = 1 \mid \mathbf{\Omega}) = \frac{N(\omega_{ij} \mid 0, v_1^2)\xi}{N(\omega_{ij} \mid 0, v_1^2)\xi + N(\omega_{ij} \mid 0, v_0^2)(1 - \xi)}.$$

- (c) **Update the knockoff latent variables (U).** This follows directly from a basic normal-normal model. We, therefore, omit the completing the square procedure. The resulting full conditional distributions of each row of the latent variable U are reported

in Section 2.2.3.

In the case of the AFT model used in the simulations, it is possible to use the exact same sampling scheme of a linear Gaussian model with an added step to update the value of the latent y_i . This update is straightforward since we do not integrate out any parameter of the model. Specifically, for subjects with $\kappa_i = 0$, the full conditional of y_i is the following Gaussian distribution

$$y_i \mid X, U, \beta, \tilde{\beta}, \mathbf{\Omega}, \sigma^2 \sim N(X_i[\beta + (I - \mathbf{\Omega}\text{diag}(s))\tilde{\beta}] + U_i\tilde{\beta}, \sigma^2)$$

truncated in the interval (c_i, ∞) .

References

- Albert, J. and Chib, S. (1993). Bayesian analysis of binary and polychotomous response data. *Journal of American Statistical Association*, 88:669–679.
- Banerjee, S. and Ghosal, S. (2015). Bayesian structure learning in graphical models. *Journal of Multivariate Analysis*, 136:147–162.
- Barber, R. F. and Candès, E. (2015). Controlling the false discovery rate via knockoffs. *The Annals of Statistics*, 43(5):2055 – 2085.
- Barber, R. F. and Candès, E. (2019). A knockoff filter for high-dimensional selective inference. *The Annals of Statistics*, 47(5):2504–2537.
- Barber, R. F., Candès, E., and Samworth, R. J. (2020). Robust inference with knockoffs. *The Annals of Statistics*, 48(3):1409 – 1431.
- Barbieri, M. M. and Berger, J. O. (2004). Optimal predictive model selection. *The Annals of Statistics*, 32(3):870 – 897.
- Bates, S., Candès, E., Janson, L., and Wang, W. (2021). Metropolized knockoff sampling. *Journal of the American Statistical Association*, 116(535):1413–1427.

- Benjamini, Y. and Hochberg, Y. (1995). Controlling the false discovery rate: A practical and powerful approach to multiple testing. *Journal of the Royal Statistical Society: Series B (Methodological)*, 57(1):289–300.
- Benjamini, Y. and Yekutieli, D. (2001). The control of the false discovery rate in multiple testing under dependency. *The Annals of Statistics*, 29(4):1165–1188.
- Benjamini, Y. and Yekutieli, D. (2005). False discovery rate-adjusted multiple confidence intervals for selected parameters. *Journal of the American Statistical Association*, 100(469):71–81.
- Berti, P., Dreassi, E., Leisen, F., Pratelli, L., and Rigo, P. (2023). New perspectives on knockoffs construction. *Journal of Statistical Planning and Inference*, 223:1–14.
- Brooks, S., Gelman, A., Jones, G., and Meng, X.-L. (2011). *Handbook of Markov Chain Monte Carlo*. CRC press.
- Brown, P. J., Vannucci, M., and Fearn, T. (1998). Multivariate bayesian variable selection and prediction. *Journal of the Royal Statistical Society: Series B (Statistical Methodology)*, 60(3):627–641.
- Candès, E., Fan, Y., Janson, L., and Lv, J. (2018). Panning for gold: ‘model-x’ knockoffs for high dimensional controlled variable selection. *Journal of the Royal Statistical Society: Series B (Statistical Methodology)*, 80(3):551–577.
- Carvalho, C. M., Polson, N. G., and Scott, J. G. (2010). The horseshoe estimator for sparse signals. *Biometrika*, 97(2):465–480.
- Castillo, I. and Roquain, É. (2020). On spike and slab empirical Bayes multiple testing. *The Annals of Statistics*, 48(5):2544–2574.
- Dai, C., Lin, B., Xing, X., and Liu, J. S. (2022). False discovery rate control via data splitting. *Journal of the American Statistical Association*, 118(544):2503–2520.
- Dreassi, E., Leisen, F., Pratelli, L., and Rigo, P. (2024). Generating knockoffs via conditional independence. *Electronic Journal of Statistics*, 18(1):119–144.

- Fan, J. and Li, R. (2001). Variable selection via nonconcave penalized likelihood and its oracle properties. *Journal of the American Statistical Association*, 96(456):1348–1360.
- Friedman, J., Hastie, T., and Tibshirani, R. (2008). Sparse inverse covariance estimation with the graphical LASSO. *Biostatistics*, 9(3):432–441.
- George, E. I. and McCulloch, R. E. (1997). Approaches for Bayesian variable selection. *Statistica Sinica*, 7(2):339–373.
- Geweke, J. (1992). Evaluating the accuracy of sampling-based approaches to the calculations of posterior moments. *Bayesian Statistics*, 4:641–649.
- Ghosal, S., Ghosh, J. K., and Van Der Vaart, A. W. (2000). Convergence rates of posterior distributions. *Annals of Statistics*, pages 500–531.
- Gu, J. and Yin, G. (2021). Bayesian knockoff filter using Gibbs sampler. *arXiv preprint arXiv:2102.05223*.
- Guindani, M., Müller, P., and Zhang, S. (2009). A Bayesian discovery procedure. *Journal of the Royal Statistical Society Series B: Statistical Methodology*, 71(5):905–925.
- Li, C. and Li, H. (2008). Network-constrained regularization and variable selection for analysis of genomic data. *Bioinformatics*, 24(9):1175–1182.
- Liu, H., Lafferty, J., and Wasserman, L. (2009). The Nonparanormal: Semiparametric estimation of high dimensional undirected graphs. *Journal of Machine Learning Research*, 10:2295–2328.
- Meinshausen, N. and Bühlmann, P. (2010). Stability selection. *Journal of the Royal Statistical Society: Series B (Statistical Methodology)*, 72(4):417–473.
- Meinshausen, N. and Bühlmann, P. (2006). High-dimensional graphs and variable selection with the lasso. *The Annals of Statistics*, 34(3):1436–1462.
- Mitchell, T. J. and Beauchamp, J. J. (1988). Bayesian variable selection in linear regression. *Journal of the American Statistical Association*, 83(404):1023–1032.

- Muller, P., Parmigiani, G., and Rice, K. (2006). FDR and Bayesian multiple comparisons rules. In *Proc. Valencia/ISBA 8th World Meeting on Bayesian Statistics, Benidorm (Alicante, Spain)*.
- Newton, M. A., Noueir, A., Sarkar, D., and Ahlquist, P. (2004). Detecting differential gene expression with a semiparametric hierarchical mixture method. *Biostatistics*, 5(2):155–176.
- Park, T. and Casella, G. (2008). The Bayesian lasso. *Journal of the American Statistical Association*, 103(482):681–686.
- Peterson, C. B., Stingo, F. C., and Vannucci, M. (2016). Joint Bayesian variable and graph selection for regression models with network-structured predictors. *Statistics in Medicine*, 35(7):1017–1031.
- Polson, N. G., Scott, J. G., and Windle, J. (2013). Bayesian inference for logistic models using Pólya–Gamma latent variables. *Journal of the American Statistical Association*, 108(504):1339–1349.
- Ren, Z., Wei, Y., and Candès, E. (2023). Derandomizing knockoffs. *Journal of the American Statistical Association*, 118(542):948–958.
- Rothman, A. J., Bickel, P. J., Levina, E., and Zhu, J. (2008). Sparse permutation invariant covariance estimation. *Electronic Journal of Statistics*, 2(none):494 – 515. Publisher: Institute of Mathematical Statistics and Bernoulli Society.
- Savitsky, T., Vannucci, M., and Sha, N. (2011). Variable selection for nonparametric Gaussian process priors: Models and computational strategies. *Statistical Science*, 26(1):130–149.
- Scott, J. G. and Berger, J. O. (2010). Bayes and empirical-Bayes multiplicity adjustment in the variable-selection problem. *The Annals of Statistics*, 38(5):2587–2619.
- Sesia, M., Sabatti, C., and Candès, E. J. (2018). Gene hunting with hidden Markov model knockoffs. *Biometrika*, 106(1):1–18.

- Sha, N., Tadesse, M. G., and Vannucci, M. (2006). Bayesian variable selection for the analysis of microarray data with censored outcomes. *Bioinformatics*, 22(18):2262–2268.
- Sha, N., Vannucci, M., Tadesse, M. G., Brown, P. J., Dragoni, I., Davies, N., Roberts, T. C., Contestabile, A., Salmon, M., Buckley, C., et al. (2004). Bayesian variable selection in multinomial probit models to identify molecular signatures of disease stage. *Biometrics*, 60(3):812–819.
- Smith, A. F. (1973). A general Bayesian linear model. *Journal of the Royal Statistical Society: Series B (Methodological)*, 35(1):67–75.
- Stamey, T. A., Kabalin, J. N., McNeal, J. E., Johnstone, I. M., Freiha, F., Redwine, E. A., and Yang, N. (1989). Prostate specific antigen in the diagnosis and treatment of adenocarcinoma of the prostate. ii. radical prostatectomy treated patients. *The Journal of urology*, 141(5):1076–1083.
- Tadesse, M. G. and Vannucci, M., editors (2021). *Handbook of Bayesian Variable Selection*. Chapman and Hall/CRC.
- Tanner, M. A. and Wong, W. H. (1987). The calculation of posterior distributions by data augmentation. *Journal of the American Statistical Association*, 82(398):528–540.
- Tibshirani, R. (1996). Regression shrinkage and selection via the lasso. *Journal of the Royal Statistical Society Series B (Statistical Methodology)*, 58(1):267–288.
- Villasenor Alva, J. A. and Estrada, E. G. (2009). A generalization of Shapiro–Wilk’s test for multivariate normality. *Communications in Statistics—Theory and Methods*, 38(11):1870–1883.
- Wang, H. (2015). Scaling It Up: Stochastic Search Structure Learning in Graphical Models. *Bayesian Analysis*, 10(2):351 – 377.
- Whittemore, A. S. (2007). A Bayesian false discovery rate for multiple testing. *Journal of Applied Statistics*, 34(1):1–9.

- Xing, X., Zhao, Z., and Liu, J. S. (2023). Controlling false discovery rate using Gaussian mirrors. *Journal of the American Statistical Association*, 118(541):222–241.
- Yap, J. K. and Gauran, I. I. M. (2023). Bayesian variable selection using knockoffs with applications to genomics. *Computational Statistics*, 38(4):1771–1790.
- Zhou, M., Li, L., Dunson, D., and Carin, L. (2012). Lognormal and gamma mixed negative binomial regression. In *Proceedings of the International Conference on Machine Learning. International Conference on Machine Learning*, pages 1343–1350. NIH Public Access.
- Zou, H. and Hastie, T. (2005). Regularization and variable selection via the elastic net. *Journal of the Royal Statistical Society: Series B (Statistical Methodology)*, 67(2):301–320.